EXPERIMENTAL STUDIES TO ADDRESS STRENGTHS OF LIMESTONE

CORES, SULFATE HEAVE PROBLEMS IN LIMESTONE

CORES AND TUNNEL LINING

BY

VIVEKANANDA CHIKYALA

PRESENTED TO THE FACULTY OF THE GRADUATE SCHOOL OF

THE UNIVERSITY OF TEXAS AT ARLINGTON IN PARTIAL FULFILLMENT

OF THE REQUIREMENTS

FOR THE DEGREE OF

MASTER OF SCIENCE IN CIVIL ENGINEERING

THE UNIVERSITY OF TEXAS AT ARLINGTON

May 2007

To my Mom, Dad, Brother and Soujanya

ABSTRACT

EXPERIMENTAL STUDIES TO ADDRESS STRENGTHS OF LIMESTONE

CORES, AND SULFATE HEAVE PROBLEMS IN LIMESTONE

CORES AND TUNNEL LINING

Publication No. _____

Vivekananda Chikyala, M.S.

The University of Texas at Arlington, 2007

Supervising Professor: Dr. Anand J. Puppala

Sulfate induced heave is a common scenario in tunnels located on sedimentary rocks containing Pyrites. Pyrite oxidation produces Gypsum which is a major source of natural sulfates. DART NC-1B tunnel is located in Dallas, north Texas. Dallas is located on sedimentary rocks with high Pyrite content and has a history of sulfate induced heave problems in several projects. In spring 2005 & 2006, the shotcrete liner in DART NC-1B tunnel showed cracking associated with water leaks. Considering the local geology and the history of the tunnel, researchers at The University of Texas at Arlington (UTA) suspected probable occurrence of sulfate induced heave and consequent formation of Ettringite. To confirm the formation of ettringite researchers at The University of Texas at Arlington designed an experimental program to address the

quality of limestone behind the tunnel lining and also to study their microstructure. In this research a comprehensive experimental program was designed to study the affects of distress on strength and structure of the limestone. A series of engineering tests including Unconfined Compression Strength tests (UCS), Indirect Tensile Strength tests (IDT or ITS) and Unconsolidated Undrained Triaxial tests (UU) were conducted to address the affects of distress on strength and deformation characteristics of limestone. Mineralogical studies including X-Ray Diffraction (XRD), Scanning Electron Microscopy (SEM) and Energy Dispersive X-Ray Micro Analysis were conducted to confirm the presence of Ettringite and also to address the micro level structural changes in distressed regions. Chemical studies were conducted to determine soluble sulfate levels in limestone cores.

All the engineering tests conducted indicated perceptible reduction in the strength and deformation characteristics of limestone cores degraded by sulfate induced heave. Mineralogical studies indicated confirmed presence of ettringite in the limestone cores. Chemical studies showed high sulfate levels in severely distressed regions. Together the experimental program designed in this research served its purpose.

TABLE OF CONTENTS

LIST OF ILLUSTRATIONS

LIST OF TABLES

CHAPTER 1

INTRODUCTION

1.1 <u>Statement of the Problem</u>

Expansive soils and rocks are those which undergo volumetric changes with moisture content fluctuations and are a major concern to researchers and practitioners in today's world (Wiggins et al., 1978; Blacklock et al., 1988). Expansions of soils and rocks occur either naturally or artificially (Serrano et al., 1988; Hunter, 1988; Basma et al., 1996). Natural expansion of soils and rocks is relatively a simple phenomenon and was elucidated by many researchers (Wiggins et al., 1978; Chen, 1993; Basma et al., 1996). In soils, natural expansion takes place due to the presence of expanding clay minerals such as presence of smectite group minerals (Basma et al., 1996). In rocks, natural expansion takes place as a result of sudden release of overburden and consequent expansion of clay minerals present in the faults and fissures of the rock mass (Serrano et al., 1988). In sulfate bearing rocks volumetric changes take place as a result of seasonal conversion of anhydrite to gypsum and vice versa in an isovolumetric conversion process (Lloret et al., 1988).

Volumetric changes taking place due to interaction of sulfate bearing soil and rock with foreign elements such as cement and lime are very complex in nature (Hunter, 1986; Serrano et al., 1988). When a sulfate bearing soil or rock comes in contact with elements such as cement and lime, will result in formation of delirious end products such

1

as ettringite and/or thaumasite which are known for their expansive behavior and lead to consequent damages to structures (Dermatas, 1992; Dermatas, 1995; Wild et al., 1999; Puppala et al., 1999).

Formation of ettringite in lime stabilized soils was first noticed in 1950s by Sherwood (1962) but it didn't receive much attention until Professor Mitchell's Terzaghi lecture in 1986 (Sherwood, 1962; Hunter, 1988). Expansive phenomenon associated with sulfate bearing soils in presence of lime was explained in detail by Hunter in his dissertation on "Lime Induced Heave in Sulfate – Bearing Clay Soil" (Hunter, 1988). There are many theories and practices developed by researchers over the time to better understand and mitigate sulfate induced heave (Mitchell et al., 1992; Dermatas, 1995). The major issue in dealing with sulfate induced heave problem is to identify the source of sulfates (Puppala et al., 1999). Occurrence of sulfates is very random and they are easily transported by ground water (Burkart et al., 1999). For years screening of sulfates was a major problem and researchers now developed non destructive mapping techniques to map sulfates present in ground (Natarajan, 2004).

There are many sources of sulfates such as industrial wastes, pollution of transportation facilities and occurrence of natural sulfate and sulfides (Chen, 1973). Among all these modes of sulfur occurrences, natural occurrence of sulfur is a major issue and is of major concern to researchers and practitioners in geotechnical engineering field.

Gypsum is the main source of sulfates in nature and is abundant in many sedimentary rocks (Berube et al., 1986). Gypsum is produced as a result of oxidation of

pyrites present in sedimentary rocks (Berube et al., 1986; Cripps et al., 1993). Gypsum formations are easily transported by ground water in a solution form through the discontinuities encountered in the rock (Evangelou et al, 1995). Some times portions of these transported gypsum formations get precipitated in the faults and fissures of host rock, the remaining unsettled deposits are transported by ground water to relatively less permeable clay soils and will result in the formation small gypsum pockets (Alonso et al., 1993; Evangelou et al, 1995). Table 1.1 presents geotechnical systems which are affected by presence of sulfates.

Table 1.1 Effects of Sulfates on Various Geotechnical Systems (Bryant et al., 2003)

Geotechnical System	Heave	Swell Pressure	Concrete Damage	Steel Corrosion	Acid Drainage
Shallow foundations, floor slabs	×	×	×	×	
Road sub-grades, road cuts and embankments	×				×
Other lightly loaded structures	×	×	×	×	
Concrete culverts	×		×		×
Concrete piles/columns	×		×		
Drilled shafts	×			×	×
Steel culverts	×			×	×
Steel structural components	×			×	×
Slope stabilization measures	×			×	×
Rock piles	×				×
Tunnels	×				×

Many researchers explained gypsum mines and pyrite bearing sedimentary rocks as the source of sulfates in north Texas (Bryan et al., 2003; Harris et al., 2004; Chavva et al., 2005).

One more aspect of sulfate induced heave is the volumetric changes taking place in sulfate bearing rocks resulting from isovolumetric conversion of anhydrite in to gypsum with large volume increases (Gens et al., 1993). Anhydrite precipitates in to gypsum with a volume increase of 62%. Structures such as tunnels and excavations built through sulfate bearing rocks often experience problems related to gypsum formation which are manifested in the form of floor heaving in tunnels, heaving of tunnel arch, cracking of tunnel lining (Madsen et al., 1995).

Delamination of tunnel lining is one more problem associated with presence of sulfates (Mehta et al., 1992; Gens et al., 1993). Sulfates present in soil, rock and water form Ettringite and/or Thaumasite with mortar (Mehta et al., 1992). This phenomenon is well known for decades (Holzer et al., 1999). The ettringite or thaumasite thus formed in mortar lead to deterioration of mortar manifested in the form of loss of strength (Mehta et al, 1992). Percolated sulfate rich water form ettringite and/or thaumasite in the tunnel lining and cause consequent delamination of the tunnel lining manifested in the form of cracks (Romer et al 2001). However, only limited research work has been carried out on this subject and limited guidance is available on how to deal with these sulfates in rocks.

1.2 DART NC-1B Tunnel Case

As mentioned earlier sulfate-induced heave, has received much national attention recently (Mitchell 1986; Little et al., 1989). On the basis of the extent of sulfate rich soils

in the United States, one can expect an increased number of reported sulfate induced heave problems in the future.

As mentioned earlier north Texas has problems with sulfate bearing rocks and soils. DART NC-1B tunnel is located near Mockingbird station in the heart of Dallas metroplex area, north Texas. For years soils and rock formations encountered in Dallas metroplex area are known for sulfate induced heave problems (Burkart et al., 1999; Puppala et al., 1999). Dallas is located on Taylor, Austin chalk, Eagle Ford shale, and Woodbine groups with occasional alluvial deposits (Richters et al., 1999). Eagle Ford shale is known to have high gypsum content and is known to create problems for various structures built in this area (Burkart et al., 1999; Puppala et al., 1999; Puppala et al., 2003). DART NC – 1B tunnel is located on uniform layers of Austin chalk with occasional Eagle Ford shale formation (Richters et al., 1999). Calcite ($CaCO_3$) is the predominant mineral in the Austin chalk (limestone) and Calcium sulfate is the major constituents of Eagle Ford shale (Freeman, 2003).

In spring 2005 and spring 2006, there was some moisture leaks located on few cracked locations observed in the shotcrete portions of DART NC-1B Tunnel. Distress locations were identified where possible delaminations of shotcrete layers and moisture leaks in the tunnel were suspected and noticed, respectively. The present research herein was performed to determine probable cause(s) for these inordinate distresses developed in DART tunnel, referred to as NC-1B tunnel.

1.3 Research Tasks

As a part of the research, rock cores near the distressed or cracked shotcrete sites in the DART tunnel were collected (by Terra-Mar, Inc.) and transported to UTA geotechnical laboratories. These samples were subjected to several tests to understand the potential causes of distress in them. The main tasks including objectives of the present research are as follows.

- The first task is to review the engineering properties of Austin Chalk and Eagle Ford shale in Dallas metroplex area. A brief history of DART NC-1B tunnel and problems associated with tunnel construction and maintenance involving underlying rock formations was documented.

- The second task of this research was to develop a theoretical frame work to understand the mechanism of the heave in the tunnel liners.

- The following research tasks are followed to accomplish the objective of this research, which is aimed at understanding the factors causing heaving distress on the shotcrete liners and then understand the strength variations of the rocks in these distress areas:

  - To asses the amount of soluble sulfate level at different distress regions and assess its effects on strength of limestone cores behind the tunnel lining.

  - Conducting engineering tests such as Unconfined Compression Strength Tests or UCS, Unconsolidated Undrained (UU) Triaxial tests

and Indirect Tensile Strength Tests or IDT to address the quality of the rock behind the tunnel lining material at various degrees of distresses.

- Conducting mineralogical studies including X-Ray Diffraction (XRD), Scanning Electron Micrograph (SEM) and EDAX to evaluate micro level structural changes in limestone cores behind the tunnel lining at various degrees of distresses.

1.4 Thesis Organization

The first chapter introduces the problems associated with sulfate bearing soils, rocks and its relevance to the current problem in DART NC -1B tunnel. It also gives details of various chapters and their contents.

The second chapter gives a thorough history and mechanism of sulfate induced heave problems in soils, rocks supporting with case studies. This was essential to the process of developing a theoretical framework upon which further experimental research work could be based.

The third chapter presents a brief review on local geology of Dallas metroplex area and DART NC-1B tunnel followed by history of DART NC-1B tunnel which includes construction and maintenance of DART NC-1B tunnel.

The fourth chapter provides details of different testing methods followed in this study. Details of engineering tests including unconfined compressive strength testing (UCS), unconsolidated undrained triaxial (UU) and indirect tensile strength testing or Brazilian split tensile strength testing (IDT or ITS) were presented at the beginning of the chapter followed by the details of test procedures and machinery used for several

mineralogical studies including X-ray diffraction studies (XRD), scanning electron microscopic studies (SEMs) and energy dispersive micro analysis studies (EDAX). UTA modified method for measuring of soluble sulfates was presented at the end of the chapter.

The fifth chapter consists of analyzing and interpreting results of engineering tests, mineralogical tests and chemical studies. It also presents correlations developed between various engineering properties of limestone cores including correlation between UCS and ITS, Point Load Index and UCS also correlation between Tangent modulus, secant modulus of limestone cores and UCS.

The sixth chapter is a summation of the conclusions drawn from engineering test results, mineralogical studies and chemical studies. Recommendations were made to prevent further propagation of distress patterns. At the end of the chapter, future research directions were also presented.

CHAPTER 2

LITERATURE REVIEW

2.1 Introduction

The main objectives of this chapter were to present a brief review on sulfate induced heave in soils and rocks and present the effects of this distress in different Civil Engineering projects. Formation and properties of Ettringite in different environments were discussed with supporting case studies. This chapter outlines problems encountered with sulfate bearing swelling rocks in different tunneling projects. Literature for this chapter was collected from libraries, internet and other projects.

2.2 Sulfate Induced Heave

Sulfate induced heave problems are catastrophic in the case of light weight structures, pavements and underground transportation and drainage facilities and also pose problems in disciplines of chemistry, geology, hydrology, environmental science and engineering (Burkart et al., 1999; Puppala et al. 1999). Oxidation and weathering of sulfur and sulfide-bearing earth material such as pyrites, shale and gypsum leads to volumetric changes, inferior engineering properties, acid production, failure of stabilization methods, and stability problems in rock and soil masses (Dubbe et al., 1999).

Sulfate attack was first noticed in Portland cement concrete and was recognized early in the 19th century (ACI, 1982; DePuy, 1994). It was proved that the reaction of

Portland cement mortar in sulfate rich environment yields delirious end products namely ettringite or thaumasite (ACI, 1982). With the advent of chemical stabilizations methods of soils i.e. stabilization of soils with foreign materials such as cement and lime, researchers came to know about the possibility sulfate problems in soils. Though sulfate induced heave in soils was observed in late 1950s, it didn't receive much attention until Prof. Mitchell's annual Terzaghi lecture (Sherwood, 1962; Mitchell, 1986). From the last few decades, sulfate induced heave problems became more predominant and attracted attention of many researchers (Mitchell, 1986; Hunter, 1988; Little et al., 1988; Dermatas, 1995; Rollings et al., 1999; Puppala et al., 1999).

Hunter (1988), in his landmark paper on "Lime Induced Heave in Sulfate - Bearing Clay Soil" was able to postulate the mechanism of reactions taking place in lime treated sulfate rich clay. According to Hunter (1988), sulfate heaving or chemical swelling is a complex mode of heaving resulting from the reaction of ground sulfates with calcium, alumina available in cement/ lime and soil/rock in the presence of moisture at specific temperature and pH conditions. According to Hunter (1988), sulfate heaving is long term scenario which often worsens the situation with elapsed time (Hunter, 1988). Unlike physical heaving, rate of chemical heaving either remains steady or worsens with time if there are sufficient amounts of ingredients present (Ferris at al., 1991). Many state DOTs in the United States are now allocating large amounts of funds to study and address the problems associated with sulfates in soils and rocks (Wiggins et al., 1978).

Clay minerals present in rocks and soils often transform in to other forms associated with changes in their structural composition and inherent physical properties

10

associated with volume changes. These volume changes are not so predominant in some mineral transformations where as they play a vital role in case of other mineral transformations such as conversion of anhydrite in to gypsum (Evangelou et al., 1995). Table 2.1 shows the volume increase in selected mineral transformations based on the assumption that altered rock was initially composed of 100 percent of the parent minerals. It is evident that in case of some minerals, transformation process produces a considerable volume increase.

Table 2.1 Volume Increase of Selected Mineral Transformations (Fasika et al., 1974; Shamburger et al., 1975; Tylor et al., 1988; Bryan et al., 2003)

Mineral Transformation		Volume Increase of Crystalline Solids
Original Mineral	New Mineral	(%)
Illite	Aluminite	8
Illite	Jarosite	10
Calcite	Gypsum	60
Pyrite	Jarosite	115
Pyrite	Anhydrous ferrous sulfate	350
Pyrite	Melanterite	536

2.2.1 Origin, Mechanism of Sulfate Induced Heave and Formation of Ettringite

Sulfate is a common mineral, exists in three phases namely solid, liquid and vapor. Soils and rocks are the example of sources for sulfates in solid state; similarly water and air are the sources of sulfates in their respective phases (Hawkins et al., 1997;

Minnesota Pollution Control Agency 1999). Sulfates (SO_4^{2-}), Sulfides (S^{1-}, S^{2-}) and organic sulfurs are the main sources of sulfate induced heave in soils and rocks and pose great danger to infrastructure facilities built on them (Hawkins et al., 1987). Figure 2.1 shows location of gypsum mines and soils with gypsum in the United States of America.

Figure 2.1 Locations of Gypsum Mines and Soils with Gypsum in the United States of America (Nettleton, 1982)

2.2.1.1 Source of Sulfates

As mentioned earlier Sulfates (SO_4^{-2}) and Sulfides (S^{-1}, S^{-2}) occur in soil, rock and can easily be transported by ground water (Skousen et al., 1996). The origin of sulfates can be traced to evaporitic deposits. Evaporitic deposits are formed by the evaporation of sea water and salt lake water followed by precipitation of salts (Zanbak et al., 1986). Anhydrite ($CaSO_4$), gypsum ($CaSO_4 \cdot 2H_2O$), halite and dolomite are the most prominent

minerals in evaporitic deposits (Zanbak et al., 1986). Reprecipitated evaporitic minerals are commonly found in upper crust in the form of evaporate, clay (e.g. gypsum mines) or fine grained clastic sediment deposits (e.g. shale and limestone) (Zanbak et al., 1986).

Gypsum and anhydrite are major constituents of many sedimentary rocks and are the major sources of sulfate that produces sulfate-induced heave in soils and rocks beneath roads, pavements, tunnels and embankments in presence of lime or cement (Thomas et al., 1987). West mentioned that sedimentary rocks are predominant in all the rock types exposed to earth's surface. 75% of all rocks exposed to earth's surface are sedimentary rocks. Pyrite (FeS_2) is a sulfide mineral abundant in many sedimentary rocks (Dubbe et al., 1997). In pyrite bearing sedimentary rocks gypsum is produced by the reaction of calcium in the rock with acid sulfate from the oxidation of pyrite (FeS_2) (Dubbe et al., 1997). Pyrites are oxidized by surface water enriched with oxygen which percolates in to the ground (Burkart et al., 1999). Equation 2.1 shows oxidation of pyrites in presence of oxygen enriched water to form ferric hydroxide and hydrogen sulfate (Harris et al., 2004).

$$4FeS_2 + 15O_2 + 14H_2O \rightarrow 4Fe\,(OH)_3 + 8H_2SO_4 \qquad\qquad 2.1$$

Once pyrite is oxidized, iron being a heavy mineral precipitates as a hydroxide and the sulfate mineral will either remains in solution and transported by ground water or oxidizes if there is sufficient calcium present to form gypsum (Bryan et al., 2003; Harris et al, 2004). Equations 2.2 and 2.3 present formation of gypsum from available sulfate mineral.

$$CaCO_3 + H_2SO_4 \rightarrow Ca^{2+} + (SO_4)^{2-} + H_2O + CO_2 \qquad\qquad 2.2$$

$$Ca^{2+} + (SO_4)^{2-} + 4\ H_2O \rightarrow CaSO_4 \cdot 2\ H_2O \hspace{4cm} 2.3$$
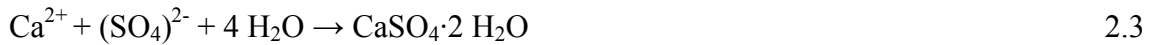
Once gypsum is formed it may move upward by capillarity or can be carried downward by infiltration or it can remain its position as an evaporite (Natarajan, 2004). Clays and rocks with their characteristic low permeability act as a reservoir for moderately soluble gypsum (Burkart et al., 1999). These gypsum deposits in soil and rocks are easily transported by ground water in solution form to other locations and are easily deposited as precipitates, hence occurrence of sulfates is very random and sulfates may occur in the form of small pockets (Puppala et al., 2005).

2.2.1.2 Mechanism of Sulfate Induced Heave and Formation of Ettringite in Soils

As mentioned in the previous section sulfates occur in soils and rocks as a result of oxidation of Pyrite. Once sulfates are present in the soils or rocks, the next phase in sulfate induced heave is the formation of ettringite ($Ca_6Al_2\ (SO_4)_3(OH)_{12} - 26H_2O$), a Hydrated Calcium Aluminum Sulfate (Hunter, 1988). Ettringite forms when a sulfate bearing soil or rock comes into contact with cement or lime in presence of water (Hunter, 1988). Form the last few decades there have been increasing number of cases of ettringite formation and consequent failure of structures at different time periods after their construction.

Perrin (1992) explained patterns of sulfate heave in Joe Pool Lake Projects, Loyd Park in Texas. In this project the sulfate were in the range of 21,000 ppm. Sulfate induced heave was evident in the form of bumps two months after stabilization with lime. Rollings et al., (1999), illustrated sulfate attack on cement stabilized sand for the case of a road constructed in Georgia. Investigations in this project revealed that well water which

is used for mixing of Portland cement was the source of sulfates. Puppala et al. (2003) reported several other case studies on sulfate heave problems in soils. In rocks, Suput et al., 2003, reported formation of Thaumasite in limestone cladding in some of the Slovenian railway tunnels. Sulfur dioxide (SO_2) released by the trains traveling in those railway tunnels was attributed as the reason for sulfate induced heave.

The above cited case studies explain the nature of randomized occurrence of sulfates. From the above case studies it can be visualized that source of sulfates can be in any medium. Figures 2.2 and 2.3 shows nature of distress in sulfate induced heave.

Due to the complexity of the problem and the increasing numbers of cases of ettringite formation and consequent damages to the structures, it is vital to elucidate formation of ettringite in sulfate bearing soils and rocks in presence of cement, lime or alumina source.

As mentioned earlier there were cases where the formation of Ettringite was established and the mechanisms were explained. Hunter (1998) in his research on "Lime Induced Heave in Sulfate – Bearing Clay Soil" explained many physicochemical reactions taking place in the formation of ettringite. According to Hunter (1998), for ettringite to form four ingredients namely Alumina (from soil/rock/cement/lime), additional calcium (cement/lime), Sulfate source (soil/rock/ground water) and water are needed at specific temperature (72°F) and pH (>10.5) environments.

Figure 2.2 Sulfate Induced Heave in Limestone Cladding of Some Slovenian Railway Tunnels (Suput et al. 2003)

Figure 2.3 Illustration of Sulfate Induced Heave (Wimsatt, 1999)

The additional calcium source and alumina source required for sulfate induced heave can either be lime, cement or soil/rock. Hence mechanism of formation of

ettringite in cement environment and lime environment are discussed separately in sections below.

2.2.1.3 Formation of Ettringite in Presence of Cement

As mentioned earlier formation of ettringite in cement concrete is well known for decades. Formation ettringite in presence of cement is attributed to the ability of cement to produce additional calcium and alumina required in the process. Portland cement is a finely divided material that results from inter grinding clinker and gypsum (Kinsey, 1987). Portland cement consists of a mixture of calcium silicates, aluminates and aluminoferrites (Greer et al., 1992). The raw materials used in manufacturing of Portland cement can be divided in to four distinctive categories: calcareous, siliceous, argillaceous, and ferriferous (Greer et al., 1992). Calcium is the highest percentage element in Portland cement and is obtained from a variety of calcareous raw materials including limestone, chalk, marl and shale. An impure limestone is known as "natural cement rock" (Kinsey, 1987). Other elements included in raw mix i.e. silicon, alumina, and iron are obtained from minerals such as sand, shale, clay and iron ore (Wang, 2003). Gypsum which is used in the finishing of manufacturing of Portland cement is excavated from quarries and mines (Wang, 2003).

Tri calcium silicate (C_3S), dicalcium silicate (C_2S), tricalcium aluminate (C_3A), and tricalcium aluminoferrite (C_4AF) are the compounds present in Portland cement in its polished form (Wang, 2003) (The abbreviation C = CaO; A = Al_2O_3; S = SiO_2; F = Fe_2O_3; H = H_2O; $\hat{S}$ = SO_3). The reactions that take place between cement and water i.e. hydration of cement are as follows.

17

$$2C_3S + 6H = C\text{-}S\text{-}H + 3Ca\,(OH)_2 \hspace{4cm} 2.3$$

$$2C_2S + 4H = C\text{-}S\text{-}H + Ca\,(OH)_2 \hspace{4cm} 2.4$$

$$2C_3A + 27H = C_4AH_{19} + C_2AH_8 \hspace{4cm} 2.5$$

$$C_3A + 3CSH_2 + 26H = C_6A\,\hat{S}_3H_{32} \text{ (ettringite)} \hspace{3cm} 2.6$$
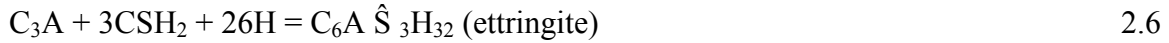
From equations 2.3 through 2.6 it can be seen that in the case of Portland cement concrete, hydration products of Portland cement provide sufficient amounts of calcium and alumina for the external sulfates to react and form ettringite. These external sulfates typically occur in the form of water used for mixing of Portland cement, crushed stone used for Portland cement concrete. Similarly in case of soils and rocks which are in contact with cement, ettringite formation takes place by 3 methods as described below.

- In the first mechanism when a sulfate bearing soil or rock comes in contact with cement, cement acts as a source for additional calcium and alumina required for the formation of ettringite and soils and rocks containing seams of pyrites and gypsum act as source for sulfates.

- In the second mechanism cement acts as a source of additional calcium required and soil or rock itself supplies additional alumina and sulfates required for ettringite formation.

- In case of sulfate bearing rocks, sulfate induced heave results from the transformation of anhydrite in to gypsum with large volume increase.

Equations shown bellow illustrates the reactions taking place between calcium, Alumina and gypsum in the formation of Ettringite.

$$Al_4Si_4O_{10}\,(OH)_8 + 4(OH)^- + 10H_2O \rightarrow 4Al\,(OH)_4^- + 4\,H_4SiO_4 \hspace{2cm} 2.7$$

$$CaSO_4 \cdot 2H_2O \rightarrow Ca_2^+ + SO4_2^- + 2H_2O \qquad\qquad 2.8$$

(Dissolution of Gypsum)

$$6Ca_2^+ + 2Al\,(OH)_4^- + 3(SO4)_2^- + 26H_2O \rightarrow CA_6\,[Al\,(OH)_6]_2 \cdot (SO4)_3.26H_2O \qquad 2.9$$
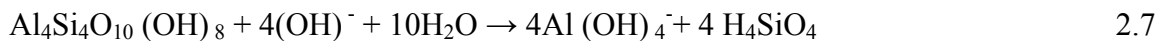
(Formation of Ettringite)

2.2.1.4 Formation of Ettringite in Presence of Lime

When lime is added to soil, pozzolanic reactions take place to form calcium silicate hydrate (CSH) and calcium aluminate hydrate (CAH) (Little et al., 2001). However when soluble sulfate is present in the soil in high concentrations; it reacts with calcium from lime and alumina from soil to form calcium-aluminate-sulfate-hydrate (CAŚH). If the concentration of sulfate is not very high, then monosulfoaluminate is formed which is not an expanding mineral and does not pose any problems to the infrastructure built on it (Hunter, 1988).

2.3 Properties of Ettringite

As mentioned earlier, formation of ettringite continues as long as there are sufficient amounts of ingredients for the reaction (Ferris et al., 1991). Once formed, ettringite induces heave either by hydration or by continuous growth of mineral itself or by both (Ferris et al., 1991). Ettringite can grow in void spaces that accommodate their growth without substantial expansion or within a dense matrix such that the soil matrix cannot accommodate the crystal growth (Natarajan, 2004). To understand complexity of ettringite formation it is vital to understand the structural composition and physical properties of ettringite.

Moore (1970) and Taylor (1974) elucidated structural properties of ettringite. According to Moor and Taylor ettringite consists of columns containing (Al (OH) $_6$)$^{3-}$. This (Al (OH) 6) $^{3-}$ are linked to neighboring Ca^{2+} ions in a polyhedra coordination system (Moore, 1970). The remaining polyhedra coordinate system is completed by water molecules (Moore, 1970). As water molecules occupy most portions (80%) of the polyhedra coordinate system, the specific gravity of ettringite is low (1.7+) (Moore, 1970). Figure 2.4 elucidates structural arrangement of calcium, alumina, and water ions in ettringite.

Ettringite is known for its expansion upon hydration (Mehta, 1974). The mechanism of expansion with hydration was studied by many researchers (Lafuma, 1952; Mikhailov, 1960; Mehta, 1974; Hunter, 1988). According to their theories, hydration of ettringite results in a volume increase of 200% of the original volume. Hence, important properties of ettringite are always connected to its expansion and swell pressures. It was established that ettringite crystals grow in void spaces in soil or rock mass with out any constraint (Mehta, 1974). On the other hand if ettringite crystals grow in dense soil or rock matrix, it exerts a pressure in the order of 241 MPa.
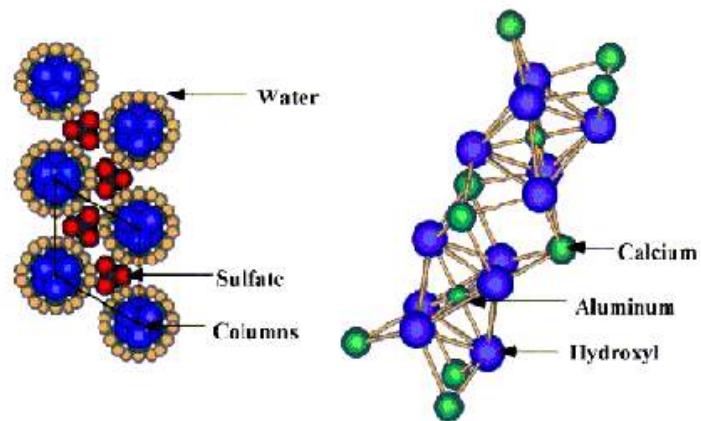
Figure 2.4 Structure of Ettringite (min.geol.uni-erlangen.del)

To understand the behavior of ettringite in different environments and to assess the swell pressure associated with ettringite hydration, researchers developed theories of stoichiometry and thermodynamics (Hunter, 1988). Some researchers used thermodynamics of geochemical reactions taking place in the expansion of ettringite and others used stoichiometric analysis to understand swelling behavior of ettringite. Researchers developed two deferent theories to explain the expansive behavior of ettringite (Cohen, 1983). According to first theory reaction, zones of ettringite formation contact others, continue growing, and mutually exert pressure. According to second theory, expansion is caused by the swelling of the ettringite particles which are of colloidal size (Cohen, 2002). Though neither of these two theories are certain about the phenomenon of swelling, there are some obvious facts, like the size of ettringite crystals is very small and ettringite growth is continuous if there are sufficient amounts of ingredients for the reaction to take place (i.e. sulfate source, additional calcium source, additional alumina source) (Wang, 2003; Puppala et al., 2005).

Mitchell (1986) reported pavement failure in Stewart Avenue, Las Vegas, Nevada and noted that the cause of failure as the formation of ettringite mineral in the treated soil. However, this paper did not address how it occurred, and what caused ettringite formation in the treated soils in detail. These questions were later addressed by Hunter (1988), who conducted a detailed study to explain the geochemistry of lime treated soils and its reactions with sulfates to cause ettringite formation. According to Hunter (1989), ettringite transforms into thaumasite at low temperatures of the order 15°C in presence of silica and carbonate (Natarajan, 2004). Thaumasite formation results in reduction of strength associated with expansion.

In many tunnels in Europe, thaumasite formation is a common phenomenon due to the prevailing low temperatures and continued exposure of rock mass to the sulfate source (Romer et al., 2001). Though sulfate levels were less in these regions thaumasite formed due to the continuous exposure to sulfate source (Romer et al., 2001). Unlike ettringite thaumasite not only induces swelling but it also weakens the rock mass. Tables 2.2 and 2.3 present general and physical properties of ettringite, respectively.

Next phase to be discussed in sulfate induced heave is the mechanism of heaving in sulfate bearing rocks resulting from isovolumetric conversion of anhydrite in to gypsum. Conversion of anhydrite in to gypsum is catastrophic in case of underground structures such as tunnels and excavations as the swell pressures resulting from these conversions are high in magnitude besides the characteristic differential movement problem associated with it.

Table 2.2 General Ettringite Information (Natarajan, 2004)

Chemical Formula :	$Ca_6Al_2(SO_4)_3(OH)_{12} \cdot 26(H_2O)$
Composition :	Molecular Weight = 1,255.11 gm
	Calcium 19.16 % Ca 26.81 % CaO
	Aluminum 4.30 % Al 8.12 % Al2O3
	Hydrogen 5.14 % H 45.93 % H2O
	Sulfur 7.66 % S 19.14 % SO3
	Oxygen 63.74 % O

Table 2.3 Physical Properties of Ettringite (Natarajan, 2004)

Cleavage	[10/10] Perfect
Color	Colorless, White
Density	1.8
Diaphaneity	Transparent
Habit	Acicular – Occurs as needle – like crystals
Hardness	2 – 2.5 –Gypsum – Fingernail
Luminescence	Non – fluorescent
Luster	Vitreous (Glassy)
Radioactivity	Not Radioactive
Magnetism	Nonmagnetic

2.4 Sulfate Heaving in Rocks Due to Isovolumetric Conversions of Gypsum and Anhydrite

As mentioned earlier gypsum is the major source of sulfates to produce sulfate induced heave. Gypsum is abundant in many sedimentary rocks (E.g. shale, limestone, and dolomite) (Jordan et al., 1989). Swelling in rocks especially in sedimentary rocks occurs due to conversion of anhydrite in to gypsum (Jordan et al., 1989). Conversion of anhydrite in to gypsum in presence of water results in a volume increase of 62% (Pina et al., 2000). Anhydrite which has orthorhombic structure gets converted into gypsum with monoclinic structure (Berdugo et al., 2005).

$\Delta V = 62\%$

Water
2 mols
36 cm^3
2H$_2$O

+

Anhydrite
1 mol
45.94 cm^3
CaSO$_4$

Gypsum
1 mol
74.69 cm^3
CaSO$_4$.2H$_2$O
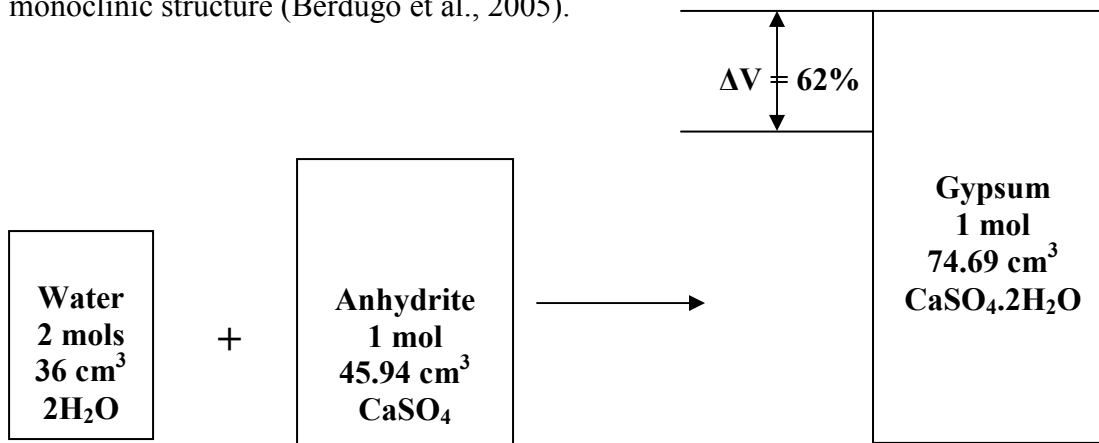
Figure 2.5 Conversion of Anhydrite to Gypsum (Modified from Berdugo et al., 2005)

Structures built on these sedimentary bed rocks often experience swelling problems due to conversion of anhydrite to gypsum. Engineering problems caused by swelling of rocks is widely recognized as there are many case studies illustrating and supporting these situations. Problems caused by sulfate bearing rocks and consequent damages (viz., heaving and swell pressures on tunnel lining) to the infrastructure associated with Asco II Nuclear power station are reported by Serrano et al.,1981, 1988,

Lloret et al., 1988, Esteban, 1990, Esteban et al., 1991, Alonso et al., 1993, Gens et al., 1993 and Alonso & Alcoverro, 2002, 2004. To illustrate the swelling phenomenon associated with sulfate bearing rocks it is vital to identify the mechanism associated with source of swelling and their triggering mechanism (Alonso et al., 2005).

For example, if a tunnel or deep excavation is constructed in a sulfate bearing rock environment, swelling takes place through two phenomenons. In the first stage, swelling is due to the sudden stress relief of the parent rock and consequent expansion of the clay impurities present in the fissures of the rock mass by absorption of water (Serrano, 1991). Swelling due to expandable clay mineral yields low swelling pressures and low swelling strains and these are suppressed with time (Serrano et al., 1991). The second phase is the swelling due to conversion of anhydrite in to gypsum associated with volume increase as mentioned in the previous section (Serrano et al., 1991). In an isovolumetric system gypsum precipitates as fast as the anhydrite dissolves with excess calcium sulfate dihydrate being either transported in aqueous solution or precipitated partially in the form of fibrous   gypsum in open discontinuities of the host rocks (Berdugo et al., 2006).

The first phase of swelling is termed as physical swelling and the second phase is termed as chemical swelling (Berdugo et al., 2005). Many tunneling projects are affected by phenomenon of chemical swelling due to the poor understanding of the number of factors influencing the mechanism of chemical swelling (Alonso et al., 2005).

Laboratory studies conducted by Grob, 1976, Esteban, 1990, Madsen et al, 1995, Abduljauwad et al, 1998, Wüst & Mclane, 2000, Berdugo, 2006 on sulfate-bearing

argillaceous rocks from different tunneling and excavation projects in Europe indicated two independent swelling mechanisms. A short term "physical swelling" due to the expansion of clay minerals and a long term "chemical swelling" due to the transformation of anhydrite into gypsum in an open system with a total volume increase of approximately 62% of the original volume as illustrated in figure 2.5 (Berdugo et al., 2006). The above mentioned lab tests indicated that the conversion of anhydrite into gypsum requires presence of certain amounts of clay mineral in the rock, which is termed as optimum clay content. According to Alonso et al., 2005, transformation of anhydrite in to gypsum with a large volume increase of 62 % is highly unlikely with out the presence of optimum clay content.

There are other theories and examples which support the impossibility of isovolumetric conversion of anhydrite in to gypsum with large (62%) volume increase (Krause et al, 1976; Madsen et al., 1995; Pina et al., 2000). Krause (1976) from the inspections of foundation materials in Wagenburg tunnel and Kappelesberg tunnel during the early 70's, confirm the validity of the isovolumetric approach. According to Krause (1976), the heaved floor in Wagenburg tunnel and Kappelesberg tunnel showed no signs of volume increase in process of complete conversion of anhydrite into gypsum except in some leached portions. Based on long–term swelling tests on various materials from the Gipskeuper and other sulfate-bearing units from Switzerland and Austria, Madsen and his coworkers presented the following hypothesis. According to their hypothesis certain amounts of clay are necessary to generate the dissolution of anhydrite and the precipitation of gypsum (Madsen and Nuesch, 1990, 1991; Madsen et al., 1995; Nuesch

et al., 1995; Nuesch and Ko, 2000). Recent contributions to the study by Pina et al., 2000, explained that the above phenomenon occurred due to epytaxial growth. When anhydrite is exposed to sulfate-rich water, gypsum generates a protective thin surface film on the anhydrite which nullifies any large volume changes (Pina et al., 2000). Some researchers suggested that the growth of gypsum crystals in porous media is dependent on super saturation gradient and hence depends on the transportation properties of the medium in which crystallization takes place (Prieto et al., 1990; Putnis et al., 1995).

From all the theories and hypothesis stated above, it is evident that swelling of sulfate bearing rocks is a complex phenomenon and it is dependent on the mineralogical composition and the structure of the rocks, as well as with the groundwater chemical composition.

One of the following reasons could be given as an isolated cause for the swelling of sulfate rich rocks:

- Osmotic phenomena and cationic exchange in clayey fractions in presence of sulfate-rich water

- Precipitation of several hydrated forms of sulfated minerals into fissures due to temperature drop of sulfate-rich water.

- Crystal growth due to evaporation of aqueous solutions into either exposed fissures or slickenside surfaces.

Figure 2.6 shows various isolated factors affecting the phenomenon associated with swelling rocks. From the reasons and explanations cited above it is obvious that the expansive phenomenon associated with conversion of anhydrite in to gypsum has potential to create problems in tunneling projects and excavation works.

```
┌─────────────────────┐                          ┌─────────────────────────┐
│ Specific Surface of │                          │ Pressure & Temperature  │
│  Anhydrite and its  │                          │   on Crystalline Phase  │
│ Interaction with    │            ╱╲            │   Changes For CaSO4     │
│      Water          │           ╱  ╲           │       system            │
│    (Bedding &       │          │    │          │  Murray (1964), Hardie  │
│  Microfissuration)  │          │TRANSFORMA│     │       (1967),          │
│   Sahores (1962)    │          │  TION    │     │  Yamamoto & Kennedy     │
└─────────────────────┘          │   OF     │     │       (1969),          │
                                 │ANHYDRITE │     │ Blount & Dickson (1973) │
                                 │  INTO    │     └─────────────────────────┘
                                 │ GYPSUM   │
                                 │IN AN OPEN│     ┌─────────────────────────┐
                                 │ SYSTEM   │     │    No reference to       │
                                 │ ΔV = 62% │     │    Groundwater           │
                                 │          │     │   Composition and        │
                                  ╲        ╱      │   Interaction with       │
                                   ╲      ╱       │   Sulfate-bearing        │
                                    ╲    ╱        │   Rock (seepage,         │
                                                  │   Geochemical            │
                                                  │   Processes …)           │
                                                  └─────────────────────────┘
              ┌──────────────────────────────────┐
              │      Relative content of clay     │
              │ Madsen & Niesch (1990, 1991),    │
              │  Madsen et al., 1995, Niiesch    │
              │  et al., 1995 and Niesch & Ko    │
              │            (2000)                 │
              └──────────────────────────────────┘
```

Figure 2.6 Schematic of Isovolumetric Conversion
(Source: Redrawn after Berdugo et al., 2006)

<u>2.5 Case Studies for Tunnel Failures in Swelling Rocks</u>

As mentioned earlier there are many case studies discussed tunnel failures in swelling rocks. Tunnels in expansive soils fail either due to excessive swell pressure exerted on tunnel lining or due to heave in the tunnel floor. Sulfate induced heave in rocks is predominant in the presence of cement, mortar and lime materials. As cement supplies sufficient amount of alumina for the ground sulfates to react, there are pronounced reactions between ground sulfates and cement resulting in the formation of ettringite and thaumasite minerals (Romer et al., 1998 & 2001).

In 1980, the International Society for Rock Mechanics formed a committee on swelling rocks to develop systematic testing procedures to address and solve problems caused by swelling rocks (Madsen, 1999). This explains the intensity and importance of the problem associated with swelling rocks. It must be noted that sulfate bearing rocks are characterized as one type of swelling rocks (Freeman, 2003).

Several papers describing tunnel case studies are reported in the literature by Alonso et al., (2005); Jethwa et al. (1977); Prommersberger et al. (1989); and Suput et al. (2003). Alonso et al. (2005) explained expansive phenomena associated with three tunnels of the new high-speed railway tunnels. Jethwa et al. (1977) explained the failure of tunnel lining caused by swelling rocks in Yamuna project, India. Prommersberger et al. (1989) explained damages caused to a tunnel in Germany due to formation of gypsum from anhydrite in a layered formation of clay/silt, marl and dolomite. Suput et al. (2003) reported formation of thaumassite in limestone fillers in a Slovenian railway tunnel.

Alonso et al. (2005) illustrated phenomenon of expansion of swelling rocks in Lilla tunnel located in Lieda-Tarragona section of the new Madrid- Barcelona high-speed railway. Lilla tunnel runs mainly through early eocenic argillaceous rocks containing anhydrite and a complex system of cross-shaped moderately dipping fibrous gypsum veins with gypsum in the veins of the parent rock (Alonso et al., 2005). The excavated portion consists of monotonic series of gypsum bearing brown argillaceous rocks (Alonso et al., 2005).

In the case of Lilla tunnel, sulfate induced heave was caused by ground water coming out from the host rock (Alonso et al., 2005). Host rock or bed rock in Lilla tunnel

29

contained high levels of sulfates in ground water. Ground water flow in Lilla tunnel was affected by the prior excavation works which resulted in the stress relief and caused the opening of slickenside surfaces and fissures. As sulfate rich ground water flow through the open discontinuities of rock it affected all the portions of the tunnel. The flow of sulfate-rich water coming from overburden triggered crystal growth in the all the portions of the tunnel and induced chemical swelling or chemical degradation.

The chemical analysis of ground water in Lilla tunnel showed that ground water contained an average sulfate content of 1783 ppm. In September 2003, just after its construction, the tunnel started showing expansions in various portion including the floor and the damages caused to the longitudinal drainage system. In December 2003, some portions of the flat slab showed heave above 600 mm with an average rate of 2 mm/day. Some sections in the invert arch showed a maximum heave of 27 mm after 10 months of their construction at a rate of 0.1mm/day. The swell pressures measured in the portions of inverted arch were high in the range of 4 to 5 MPa.

 Tunnel linings generally protect the bed rock from mechanical disintegration, leaching and to avoid the percolation of ground water in to the tunnel (Romer et al., 1998 & 2001; Alonso et al., 2005). Tunnel linings are often attacked by the ground sulfates which percolate through the cracks and joints present in the parent rock. Leaching of the tunnel lining starts from the contact surface of tunnel lining and the bedrock and progresses towards the centre (Romer, 1998). Figure 2.7 shows the percolation of ground water in to the tunnel lining and subsequent lack of adhesion between liner materials and tunnel surface (bed rock surface).
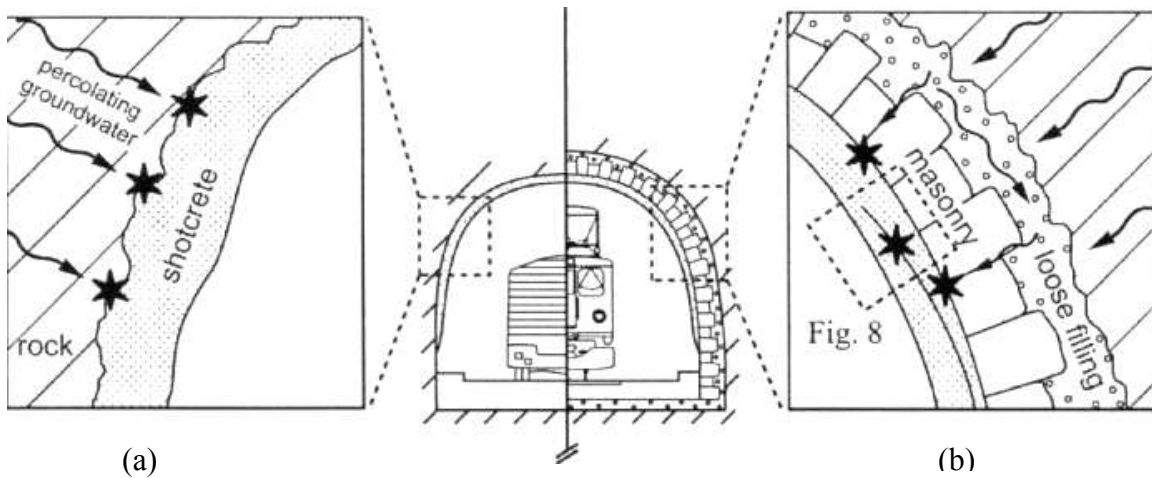
Figure 2.7 Mechanism of Percolation of Sulfate Rich Water Through the Tunnel
Lining and Consequent Damages to Tunnel Lining in (a) Buen Road Tunnel
and (b) Koblenz Railway Tunnel in Europe (Romer et al., 2001)

Some regions of shotcrete linings in tunnels are often in contact with percolating ground water for a prolonged time which makes them saturated in specific zones. If the ground water percolating through the open spaces contains considerable amounts of sulfates, they attack the contact surface of the shortcrete lining and bedrock surface leading to detachment of shotcrete from the tunnel surface due to reduction of adhesion between these two materials.

As only certain zones of shotcrete lining are saturated due to the percolation of water in specified zones, delamination of shortcrete layer takes place only in those regions. This phenomenon is referred to as chemical zonation (Romer et al., 1998). As ground water show different compositions in different regions, the degradation of shotcrete appears in zones (Romer et al., 1998).

Though sulfate levels are low in ground water, prolonged exposure of shotcrete material to sulfates will cause delamination of shotcrete material through the formation of ettringite or thaumasite (Mehta et al., 1992). Figure 2.8 shows the mechanism of degradation of Shotcrete material in the presence of sulfate rich water.
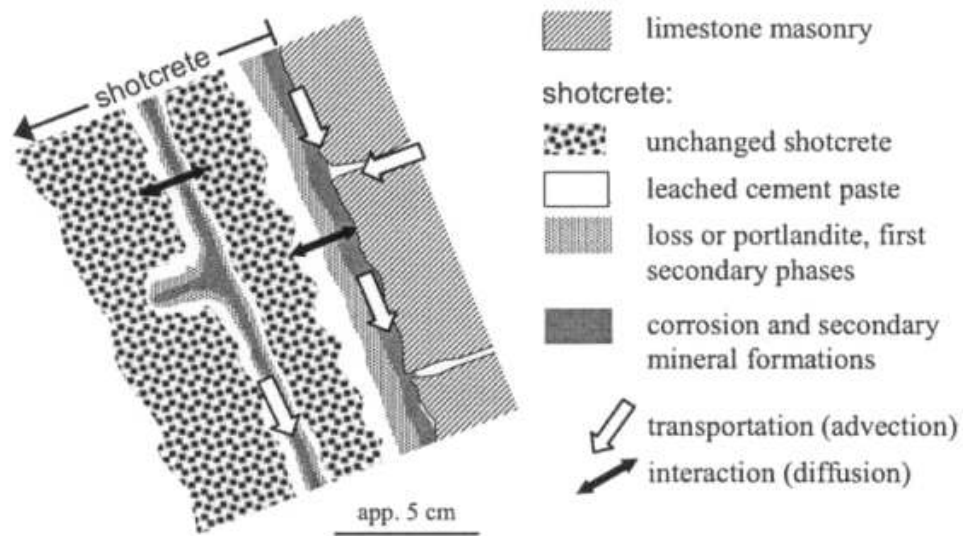
Figure 2.8 Mechanism of Degradation of Shotcrete Material in Sulfate Rich Environment
(Romer et al., 1998)

As mentioned earlier in the present case of DART NC-1B tunnel in this research, there were regions with localized delaminations of shotcrete tunnel lining were observed. These delamination patterns were attributed to the sulfate induced heave. Figure 2.9 shows patterns of delamination in some of the tunnels in Europe which were Similar to patterns observed in case DART NC-1B tunnel.
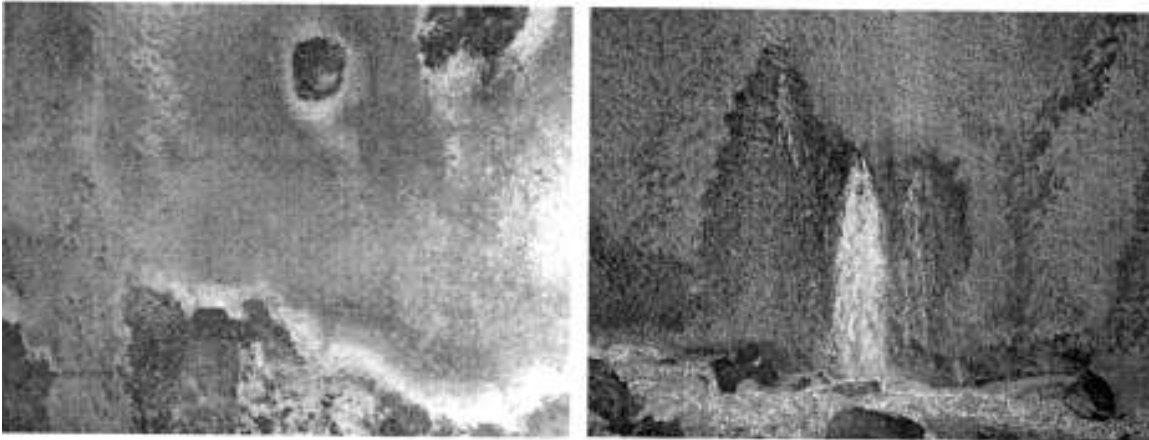
(a)   (b)

Figure 2.9 Delamination of Shotcrete Lining in Some of the Tunnels in Europe Due to Presence of Sulfates (a) Percolation of Ground Water, (b) Formation of Sulfide Rich Matter (Romer et al., 1998)

2.6 Summary

This chapter gives a brief history about the problems associated with sulfate heaving. A review on source and occurrence of sulfates were presented with appropriate case studies. Formation and properties of ettringite have been discussed with an emphasis on behaviors of sulfate rich soils and rocks in the presence of alumina source i.e. cement and lime additives. Isovolumetric conversion of anhydrite into gypsum in sulfate bearing rocks was discussed with an insight into the mechanism of isovolumetric conversion and the factors affecting it. At the end effects of sulfates on tunnel linings and consequent delamination of tunnel lining were presented supporting with case studies.

CHAPTER 3

SITE GEOLOGY AND HISTORY

3.1 Introduction

The main objective of this chapter is to presents the details of local geology of Dallas metroplex supporting with geological maps. Emphasis has been laid on the details of geological formations encountered in DART NC-1b tunnel site. The location and construction sequence of DART NC-1B tunnel are documented along with the engineering properties of geological formations encountered at the specific site location.

3.2 Local Geology of DART NC-1B Tunnel

Sedimentary rocks are predominant in all the rock types exposed to earth's surface. 75% of all rocks exposed to earth's surface are sedimentary rocks. It is vital for engineers to study and better understand the behavior of sedimentary rocks. City of Dallas metroplex is underlain by sedimentary rocks which belong to Cretaceous period (Kim, 2003). The strata dips (2º) gently to the southeast into the subsurface due to the structural changes that occurred after the strata were deposited (Kim, 2003). The outcroppings of Dallas area consists of Taylor, Austin chalk, Eagle Ford shale, and Woodbine groups with occasional alluvial deposits (Richters et al., 1999). Figure 3.1 shows geology of Dallas metroplex area on a regional scale
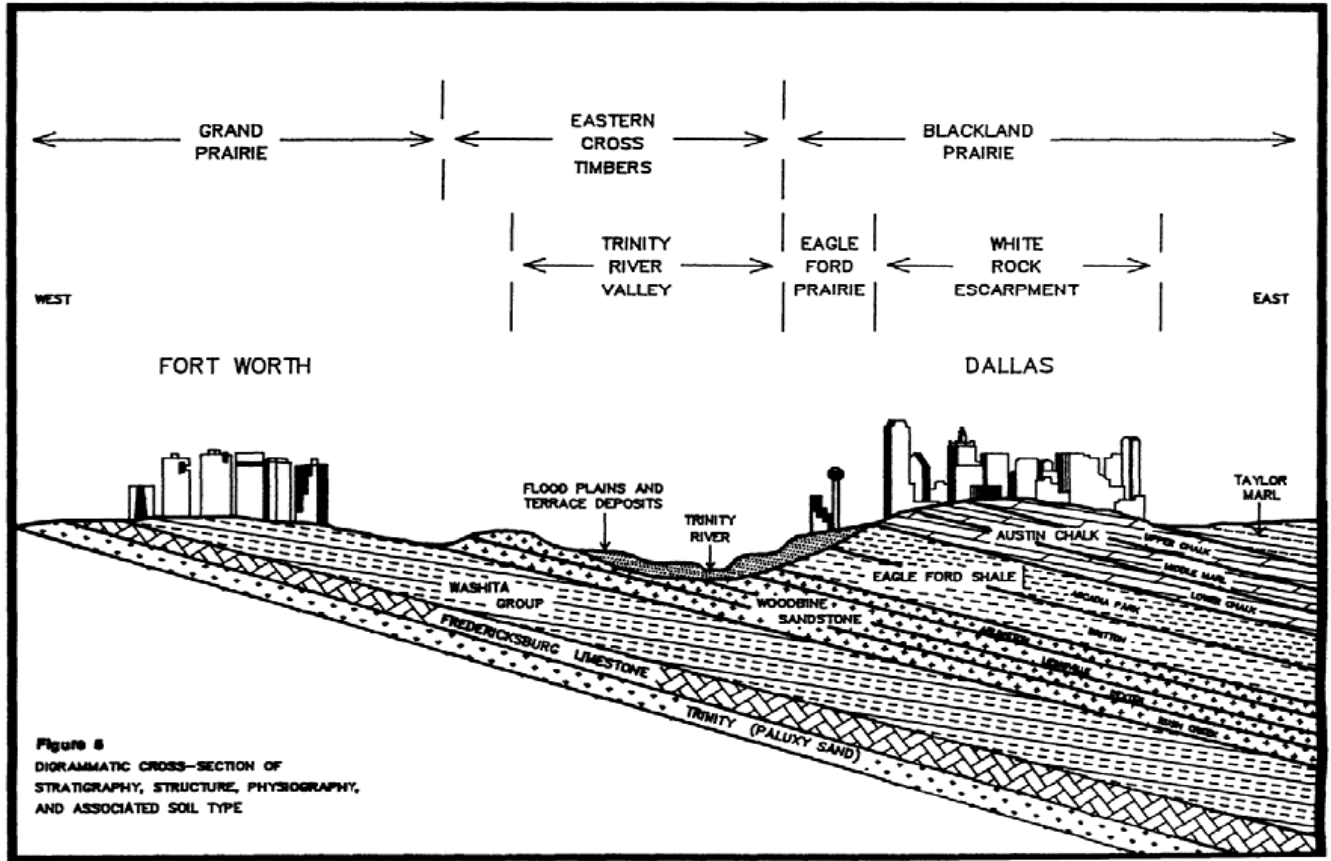
Figure 3.1 Geology of Dallas Metroplex on a Regional Scale
(Dallas Geological Society)

DART tunnel was constructed with an aim of reducing traffic congestions in downtown Dallas (www.dart.org). In 1990 DART initiated a project for light rail system which included design and construction of 32 km light rail system. 5.2 km of this light rail section was identified to be constructed below grade either in the form of open excavation or as a mined tunnel (Richters et al., 1999). Finally, it was decided to construct the first 1.2 km as a mined tunnel and the remaining 4 km as an open excavation. During the construction of DART tunnel designers took advantage of geological exploration of previous projects and ongoing projects that were constructed in Dallas (Richter's et al., 1999).

According to DART's initial master plan, light rail system was to be constructed in tandem with the reconstruction of US 75 highway. The south end of the tunnel was constructed bellow grade of interchange between Woodall Rodgers freeway and US 75 and the north end of the tunnel was located about 9 m north of Mocking bird lane and had about 8m of cover between tunnel crown and pavement. According to Wallis, 1992, there were at least seven geotechnical site investigation performed either by DART or the US 75 reconstruction crew. DART designers took advantage of all the pertinent data available from the records and recommended additional geotechnical site explorations to fully explore the site for the construction of 5.2 km of underground rail system (Richter's et al., 1999).

Details of geotechnical profile of site consisted of uniform layers of Austin chalk or occasional Eagle Ford shale overlain by recent alluvial deposits and bentonite seams (Richter's et al., 1999). Top portion of alluvial deposits are primarily dark gray to tan,

calcareous clay, silt and sand. The bottom portion or basal consisted of stratified water bearing clay, sands and gravel (Richter's et al., 1999). Ground water table was at a depth of about 7.5m. Bentonite seams prevented water from percolating to the underlying Austin chalk.

Many tunneling projects built through shale and mudstone had problems with Isovolumetric conversion of anhydrite into gypsum and consequent heaving. Eagle ford shale is known to create many heave related problems in the Dallas metroplex with its inferior engineering properties and high pyrites content (Harris, 2004). Eagle Ford shale is marine shale with calcareous and non calcareous Montomorillonite clay mineral (Natarajan, 2004).

To avoid the complications associated with Eagle Ford shale i.e. swelling due to moisture fluctuations, it was decided to build the tunnel through Austin chalk and avoid Eagle Ford formation (Richter's et al., 1999).

Though the Austin chalk encountered in this area is uniform and has good engineering properties. As a typical characteristic of lime stones, it has minor and major cracks (Proctor et al., 1968). As mapped by US 75 reconstruction crew, there were series of single, tight faults with displacements up to about 1.5 m (PB/MK, 1992, Richter's et al., 1999). One major fault was encountered in Austin chalk of DART tunnel with characteristics of a shear zone, slickenside and high permeability. During the construction ground water started flowing from this fault. To avoid flow of ground water in to the tunnel a detail using filter fabric was provided to direct the seepage into tunnel invert (Richter's et al., 1Bentonite seems which usually pose problems with their expansive

37

nature were proved to be advantageous in DART tunnel (Richter's et al., 1999). The Bentonite seems were located sufficiently high above the tunnel crown they acted as a water barrier and disrupted percolation of water in to the underlying rock mass.

3.3 Typical Properties of Austin Chalk and Eagle Ford Shale Encountered in the Site

The DART tunnel mentioned here passes through Austin chalk, which exhibits uniform engineering properties. Eagle ford shale was also identified at certain locations of the tunnel. Table 3.1 presents properties of both shales.

Table 3.1 Geological and Engineering Properties of the Site (Richters et al., 1999)

Stratum	Classification	Total Unit Weight (Kg/m^3)	Friction Angle (deg.)	Cohesion (kPa)	Description
Soil Strata					
Upper Terrace	CL	2.08	15	143	Deposits with occasional silt, sand gravel and lime deposits
	CH	2.05	17	72	
Lowe Terrace	Non-cohesive	2.1	35	0	Sand coarser with depth, gravel pockets in sand
Austin Chalk	Residual Clay	1.9	5	86	Limey CL to CH w/ occasional Lime
Unweathered Austin Chalk					
Water Content (%)	Range Mean	2 – 20 11			Austin Chalk Limestone fresh Bluish gray
Unit Dry Weight (g/cm^3)	Mean Std. Deviation	2.1 0.13			
Unconfined Compression (MPa)	Mean Std. Deviation	17.5 4.0			
Weathered Austin Chalk					

Table 3.1-Continued

Water Content (%)	Range	2- 29	Austin Chalk Limestone severely to highly weathered
	Mean	13	
Unit Dry Weight (g/cm^3)	Mean	1.9	
	Std. Deviation	0.10	
Unconfined Compression Strength (MPa)	Mean	6.3	
	Std. Deviation	2.8	
Eagle Ford Shale			
Water Content (%)	Range	13 -17	Dark bluish gray black shale
	Mean	15	
Unit Dry Weight (g/cm^3)	Mean	1.9	
Unconfined Compression (MPa)	Range	1.8 – 3.3	
	Std. Deviation	2.3	

In the next chapter, properties of these Austin chalk and Eagle Ford formations are compared with the standard engineering properties of these formations in this region and are classified accordingly with respect to their strength properties.

3.4 Details of Tunnel Lining

As mentioned earlier tunneling is necessary for accounting for the mechanical disintegration of bed rock. In DART tunnel mentioned here in, a 230-mm unreinforced final tunnel lining was provided to support the tunnel. During the construction, a 100-mm thick fiber reinforced tunnel lining was provided to mitigate the weathering and unraveling of Austin chalk. To control the ground water flow through the faults in Austin chalk, a 230-mm thick cast–in- place concrete liner was provided in some locations.

3.5 DART Tunnel History

On June14 of 1996 DART started operating light rail system. The tunnel was constructed within the allocated budget and as per the schedule.

Figure 3.2 Picture of DART Tunnel Mined Portion

In April 1996, a portion of DART tunnel which was constructed as a mined portion started developing a few water leaks at several construction joints. Although the tunnel was completely lined with a waterproof membrane prior to the final concrete pours, the leaks were still occurring. DART and the engineering group proposed to inject the leaking with suitable injecting materials. The materials used for injection varied in accordance with the severity of the leaks. DuroRapid, a fast sealing, dense rubber like substance was used in areas with severe leaking (flowing water) (www.dart.org). In areas with moderate water leaks, characterized as the areas that were only weeping or just damp, BBZ injection resin was used. Duroseal Inject was the BBZ Injection Resin used in joints or cracks that were only weeping or just damp. Unfortunately there is no

published information available about the exact location of these water leaks from the construction joints.

3.6 Description of Present Problem

In spring 2006, a few distress locations with water leaks were observed in the mined tunnel. Distress locations were identified where possible delaminations of shotcrete layers and moisture leaks in the tunnel were suspected and noticed, respectively. These areas are mainly focused in the present research.

As a part of the research, rock cores near the distressed sites in the DART tunnel were collected (by Terra-Mar, Inc.) and transported to UTA geotechnical laboratories. These samples were subjected to several tests to understand the potential causes of distress in them.
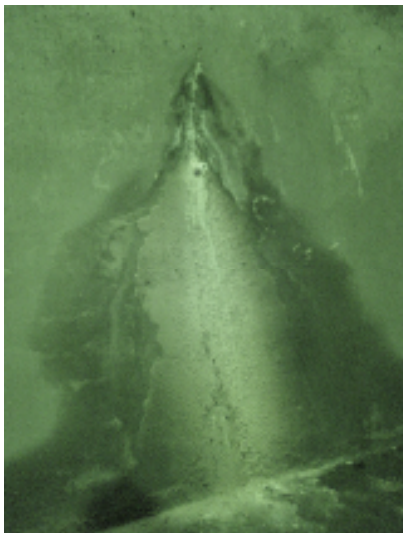
(a)   (b)

Figure 3.3 Delamination of Tunnel Lining DART NC-1B Tunnel, (a) Percolation of Water Through the Tunnel Lining, (b) Formation of White Powder Like Substance

In this research, the main emphasis was to address possible causes of distress in limestone rock formations and then evaluate the effects of this distress on macro engineering properties of the limestone material located behind the lining. One of the potential causes of distress in Limestone could be the formation of ettringite and thaumasite minerals, which are known to induce cracking when they are hydrated and expanded (Hunter, 1986). In order to study this, several powdered samples were collected from distress regions where white powder type substance known as Gypsum was noted. These samples were subjected to mineralogical studies including X-Ray Diffraction (XRD) and Scanning Electron Micrograph (SEM) studies. Chemical studies were also conducted to assess whether the powder form substance observed on the tunnel lining belongs to Gypsum or calcium sulfates. Another research objective is to address the quality of the rock behind the tunnel lining material at various degrees of distresses

3.7 Summary

Dallas metroplex is underlain by sedimentary rocks of cretaceous age with a slope gently dipping (2°) towards south east. DART NC-1B tunnel, which is located in Dallas on a uniform layer of Austin chalk with occasional eagle ford shale formation. Construction of DART light road system was started in 1991 and was opened to traffic in 1996. Immediately after construction i.e. in April 1996, the mined portion of DART tunnel showed water leaks from the construction joints which were later fixed. In spring 2005 and 2006, the mined portion of the DART tunnel developed some distresses manifested in the form of cracking in shotcrete tunnel lining along with leaking of water from some of the distressed regions.

CHAPTER 4

EXPERIMENTAL PROGRAM

4.1 Introduction

This chapter outlines the details of sampling methods and the details of different tests conducted on limestone cores and powdered material observed at various distressed regions located in DART NC – 1B tunnel. Details of cracking patterns observed various distress regions have been documented along with supporting photographs. Details of various engineering test including Unconfined Compression Strength test (UCS), Unconsolidated Undrained Triaxials (UU) and Indirect Tensile Strength (ITS or ITD) are documented followed by the details of procedures and machinery used in mineralogical testing which includes X-Ray Diffraction (XRD), Scanning Electron Microscopy (SEM) and Energy Dispersive X-Ray Micro Analysis (EDAX). At the end of the chapter details of chemical studies for soluble sulfate measurements are presented.

4.2 Identification of Distress Patterns

As mentioned earlier the main emphasis of this study was to determine the probable cause for the distress patterns developed in the tunnel. Three tunnel locations were selected such that they represent regions of high, medium and low or no possible distress areas. Details of these distress station locations were presented in the Terra-Mar,

Inc. reports (Table 4.1). It should be mentioned that these distress are associated with the liner crackings noted with possible moisture leak locations as shown in Figure 4.1. Traces of white powder material could also be found on the same location.

(a)   (b)

(c)
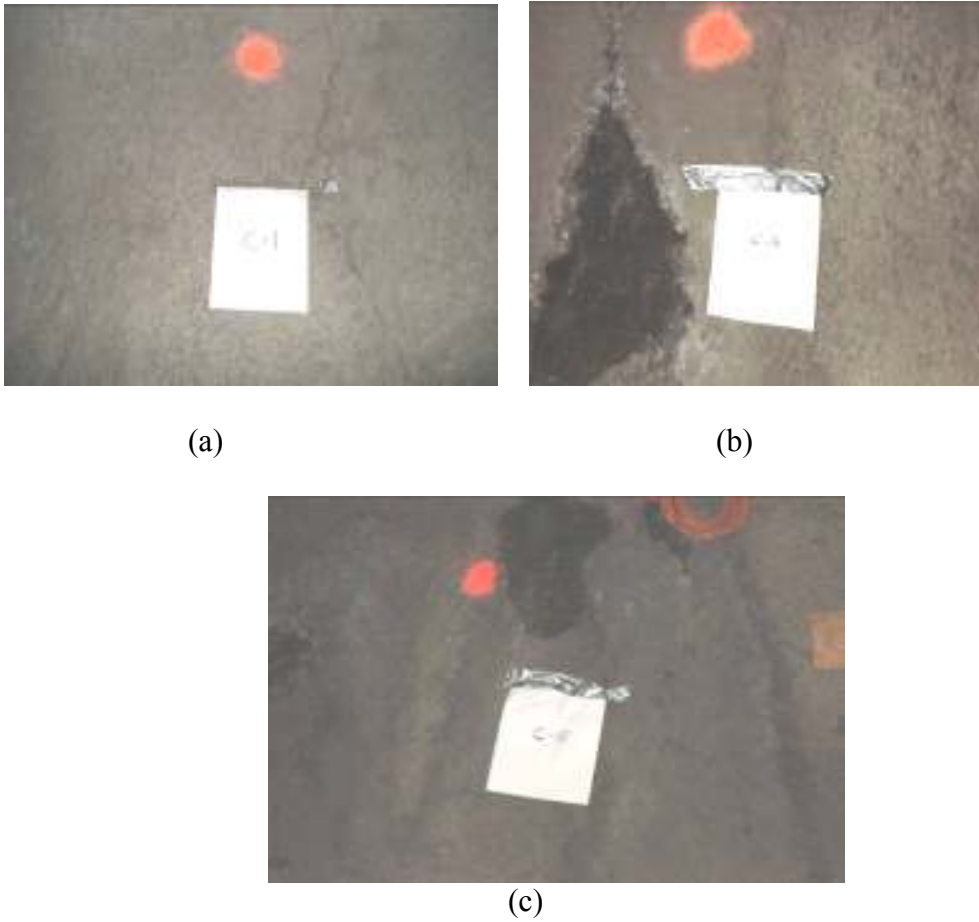
Figure 4.1 Heave Distress Locations Inside the Tunnel Site (a) Low Distress Area
(b) Medium Distress Area (c) High Distress Area

Table 4.1 Sample Notation and Location

Classification	Notation	Location
Low Distress Area	C-1, C-2	Station 357.20
Medium Distress Area	C-3, C-4	Station 357.60
High Distress Area	C-5, C-6	Station 358.20

Rock cores from the distress sites were then collected and were later subjected to engineering tests which included indirect tensile strength tests, unconfined compression strength tests, and unconsolidated undrained triaxial tests at a confinement of 150 kPa. Both strength and stiffness properties were determined and these results were compared with respect to visual distress ratings at the site. Additionally, the formation of ettringite minerals and their possible links with the distress located at the tunnel stations are explained

<u>4.3 Field Sampling</u>

4.3.1 Rock Core Sampling

Approximately, six coring locations selected for field sampling are presented in Table 4.1. Two 3 in. diameter rock cores were sampled at each location, which are spaced at 20 ft apart with 2 ft long samples Carbide rock core barrels were used for sample coring operations. After coring was completed, core holes were filled with quick setting concrete and then sealed. Moisture content is a vital factor affecting the strength of a rock, hence samples for carefully wrapped in aluminum foils to preserve the in situ moisture conditions and were transported to Terra-Mar, Inc laboratory.

4.3.2 Powder Sampling

Powdered form material was obtained from the cracks in tunnel lining and from the areas where water leaking was observed by scratching the surficial material with a metal bar. Figure 4.2 shows a typical coring operation for retrieving rock samples. After field sampling, samples were transported to UTA geotechnical laboratory for further testing. A series of laboratory tests were performed on rock core samples and powdered samples to evaluate the sulfate heave and to assess the effect of distress on quality of rock materials. Mineralogical studies such as X-ray Diffraction and Scanning Electron Microscopic studies were conducted on powdered samples to address the presence of sulfates and potential sulfate heaving problems behind the tunnel lining. Engineering tests conducted in this research include unconfined compression strength (UCS), indirect tensile strength (IDT), unconfined undrained triaxial (UU) tests. Details of these tests are discussed in subsequent sections

Figure 4.2 Coring of Rock Samples Using Carbide Rock Core Barrel

4.4 Engineering Tests

4.4.1 Unconfined Compression Strength Tests (UCS)

Compressive strength of rock is quantitative measure of quality of the rock. The apparatus used for UCS testing was an electronic-servo controlled MTS testing machine with a loading capacity of 220 kips. Loading data and other test parameters were recorded with a computer based data acquisition system, and the data is subsequently reduced and analyzed with a customized spreadsheet program.

Several standard testing methods are available for compressive strength testing of rocks and soils. In the present research, ASTM D-2938 test method was followed for the UCS tests on rocks. Compressive strength of rock as determined by the UCS method could be indirectly used to estimate elastic moduli of the intact rocks. If the parent rock contains faults, fissures and other anomalies such as heave related ettringite compounds, then the rock material will yield low strength properties. In such cases, these correlations need to be considered with sound engineering judgment.

In UCS test, cylindrical rock specimens were tested without lateral confinement. The test procedure is similar to the unconfined compression test for soils and concrete. An aspect ratio of 2 was used for each sample with flat, smooth, and parallel ends cut perpendicular to the cylinder axis. The apparatus typically consists of a loading frame, LVDTs to measure axial and lateral deformation of the sample with increasing load. For each distress location, two samples were tested and average UCS is reported. Figure 4.3 shows the system used for unconfined compressive strength testing.
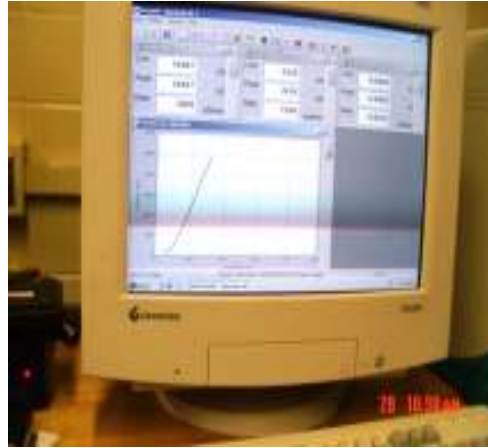
(a)	(b)

Figure 4.3 UCS Test Setup and Details (a) UCS Testing Machine (b) Data Acquisition System

Figure 4.4 Sample Loaded to Failure in UCS Test

In UCS testing, sample was placed in the loading frame and the load was increased to the failure and axial deformations were measured. Load versus axial

deformation graphs obtained in computer program was used to plot stress-strain curves using an MS excel work sheet (as the sample dimensions are known).

4.4.2 Indirect Tensile Strength (ITS) Test

Measuring the direct uniaxial tensile strength of a rock is hard and expensive task due to the need to use clamp system. Hence, researchers often use indirect methods and correlations to measure tensile strength of a rock. An indirect tensile strength test also known as Brazilian split tensile strength test has been used to determine the tensile strength of the rocks. In this research, the indirect tensile strength properties of the rock cores were measured using ASTM D3967 method. In indirect tensile strength (ITS) test, an aspect ratio of 1 was used with both height and diameter of sample being close to 3 in. Samples were placed in a compression loading machine with the load platens situated diametrically across the specimen. The maximum load (P) to fracture the specimen is recorded and used to calculate the split tensile strength. For ITS testing, the same loading unit was used. Figures 4.5 and 4.6 present the ITS test in progress. Figure 4.6 (a) presents a vertical crack across the rock specimen, splitting the specimen in the ITS method.

Figure 4.5 Loading Frame and Sample for IDT

<div align="center">(a)   (b)</div>

Figure 4.6 (a) Development of First Crack in IDT, (b) Sample at Failure in IDT

The following Equation 4.1 was used to calculate the splitting tensile strength of the rock specimen from the load versus deformation curve obtained from the IDT method:

$$\sigma = \frac{2 \times P}{\pi \times L \times D}$$

4.1

Where

σ is splitting tensile strength in MPa (psi)

P is the maximum applied load indicated by the testing machine (N or lbf)

L is the thickness or length of the specimen, mm (or in.)

D is the diameter of the specimen, mm (or in.)

4.4.3 Unconsolidated Undrained (UU) Triaxial Test

Shear strength consisting of cohesion and friction angle characteristics is an important property of a rock material. A series of unconsolidated undrained compression tests were typically conducted to determine the shear strength of the rock. ASTM D-

2664 test procedure was typically followed in determining the shear strength of rock. This type of test simulates the behavior of rock under the ground as there is a confining pressure applied in the test to simulate the overburden loading. Stress strains plots were made and analyzed to estimate the undrained shear strength of the rock, which was equivalent to the deviatoric stress applied to the specimen at which the rock specimen has either yielded or failed. In this research, a confining pressure of 150 kPa or 21 psi was applied. The aspect ratio of the rock specimen was 2.

Initially the rock cores were placed in the triaxial cell. An initial confining pressure (σ_3) of 21 psi was then applied to the sample in the triaxial cell. The cell was placed under the loading unit and then the cell was moved at a constant strain rate. The final load applied on the specimen at failure was recorded and used as a deviatoric stress (σ_d). The triaxial setup used in this research was shown in Figure 4.7. The same loading setup was used for UCS tests.

Figure 4.7 Initial Application of Confinement in UU Triaxial

Figure 4.8 shows the application of load on to the rock specimen placed in a triaxial cell utilizing a 400 kip tensile compression machine. During the testing, the data was recorded in a data acquisition oriented computer system and the collected data was analyzed and then reduced using a customized spread sheet. Figure 4.8 shows a typical rock specimen immediately after the failure.

Figure 4.8 Loading of Specimen in 400 kip Tensile Compression Machine

Figure 4.9 UU Triaxial Specimen Loaded to Failure

4.5 Mineralogical Tests

As mentioned earlier, cracks were detected on the tunnel lining material. Water leaks from the cracked areas lead to distress in the microstructure of rocks and shortcrete material, which could be attributed to the formation of sulfate, based mineral compounds such as Ettringite and Thaumasite. Hence, a series of X-ray diffraction and scanning electron microscopic studies were conducted to assess the formation of any sulfate rich compounds. Details of these tests are given in the following.

4.5.1 X-Ray Diffraction Studies (XRD)

X-ray diffraction (XRD) studies were conducted on selected rock core powder samples and powdered specimens collected from the field to verify ettringite formation. In X-ray diffraction test, powdered samples were subjected to an intense X-ray beam and the d-spacing of diffracted waves were then measured. Prior to the X-ray diffraction test, rock samples were air dried and crushed such that most of the material passes through No. 200 sieve. Oven drying is not a preferable method since it may change the engineering properties of the rock (Chew et al. 2004).

The powdered sample was placed in a sample holder and X-ray diffraction studies were carried out using a CuKα D-500 X-ray diffractometer with an input voltage of 30 kV and current of 30 mA. A continuous scan mode and a scan rate of 2-degrees per minute were selected. Figure 4.10 shows the sequence of X-ray diffraction testing. Bragg angles given by Brown (1961) and Mitchell (1992) were used for mineralogical analysis of X-ray diffraction data.

Figure 4.11 presents the pattern of Bragg angles observed in D-500 computer graph. Figure 4.11 presents a plot between scan angle and intensity counts of reflected X-ray. Peaks for a particular scan angle and intensity counts, when matched with those of Ettringite and Thaumasite minerals, indicate the presence of distress causing minerals like ettringite or thaumasite.

(a)

(b)

Figure 4.10 (a) Sample for XRD, (b) Cukα D-500 Machine
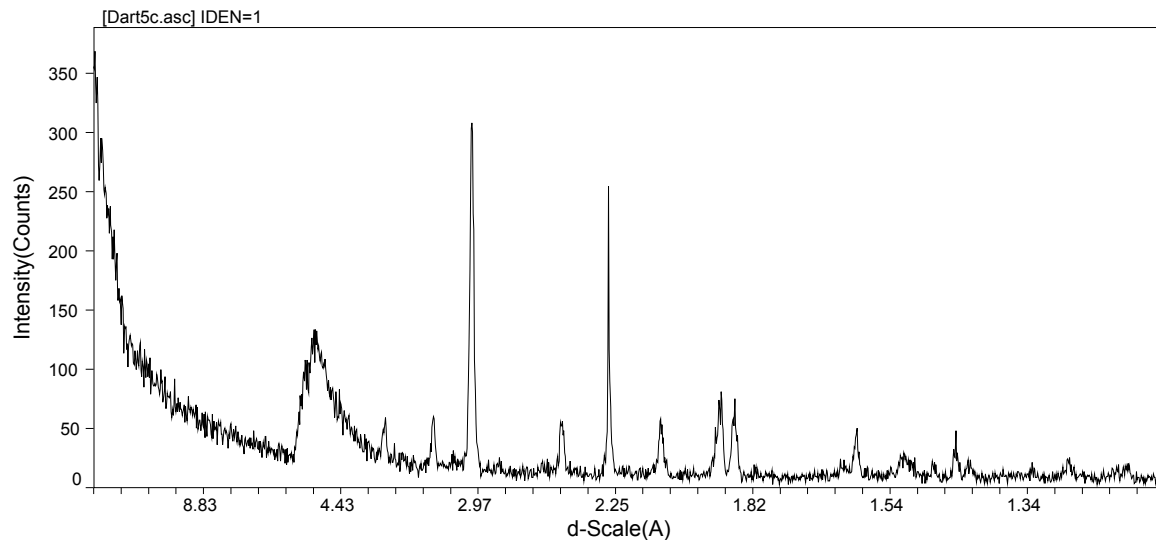
Figure 4.11 Plot Between Bragg Angle and Intensity Count

4.5.2 Scanning Electron Microscopy (SEM)

Scanning electron microscope studies were conducted on rock powdered samples using a scanning microscope (SEM). The Scanning Electron Microscope (SEM) uses electrons rather than light to form an image. The soil samples were air dried and crushed prior to SEM analysis. The broken samples were then placed on an aluminum stub using a double-sided carbon conducting tape. The SEM as shown in Figure 4.12 allows a large amount of the sample to be in focus at one time and it produces images of high resolution, which means that closely spaced features can be examined at a high magnification level.

Preparation of the samples is relatively easy since most SEMs require the sample to be conductive. Rock is not as conductive as metals; hence coating with a conducting material was necessary for quality SEM analysis. Coating of the sample was done with carbon, copper or silver. Coating of the sample was carried out in a vacuum operated

coating machine at an operating current of 100-mA and a pressure of 0.001-mtorr (Figure 4.13). The combination of higher magnification, larger depth of focus, greater resolution, and ease of sample observation makes the SEM one of the most heavily used instruments in research areas today. After coating the samples as shown in Figure 4.12, the samples were placed SEM machine and analyzed with an accelerating voltage of 20KV and working distance less than 30. The SEM results are discussed in detail in the 'analysis of results' section.

Figure 4.12 Scanning Electron Microscope (SEM) Assembly

Figure 4.13 Sample Coating in SEM

4.5.3 *Measurement of Soluble Sulfates*

The soluble sulfate content in the soil is an important test property that is known to assess the sulfate heaving process in chemically treated soils. The method used in this research to measure soluble sulfates is a modified procedure from the standard gravimetric method outlined in the seventeenth edition of Standard Methods for the Examination of Water and Wastewater. Figure 4.14 presents the measurement procedure in a flow chart format.

The water extraction ratio used in this method was 1:10; by which 10 grams of dried soil was diluted with 100 mL of distilled water. The extraction of the solution was obtained by centrifuging with the speed of 14,000 rpm. The pH values of the solution were controlled within the range of 5 to 7 by Hydrochloric acid. Barium Chloride ($BaCl_2$)

was then added in the boiling solution to bring out sulfate in the form of Barite ($BaSO_4$). The solution was placed in an 85°C oven for 12 hours to continue the digestion process in which precipitation takes place to obtain Barite by gravimetric process. The barite precipitated from this process was calculated to obtain the soluble sulfate contents in the soil samples.

Puppala et al. (2002) used a smaller pore size filter of 0.1 μm and higher speed of centrifuging of 14000 rpm with longer time in order to segregate the small particles from the solution. This modified method provided results that match with ion chromatography measurements. Hence, this method was used in the present research.
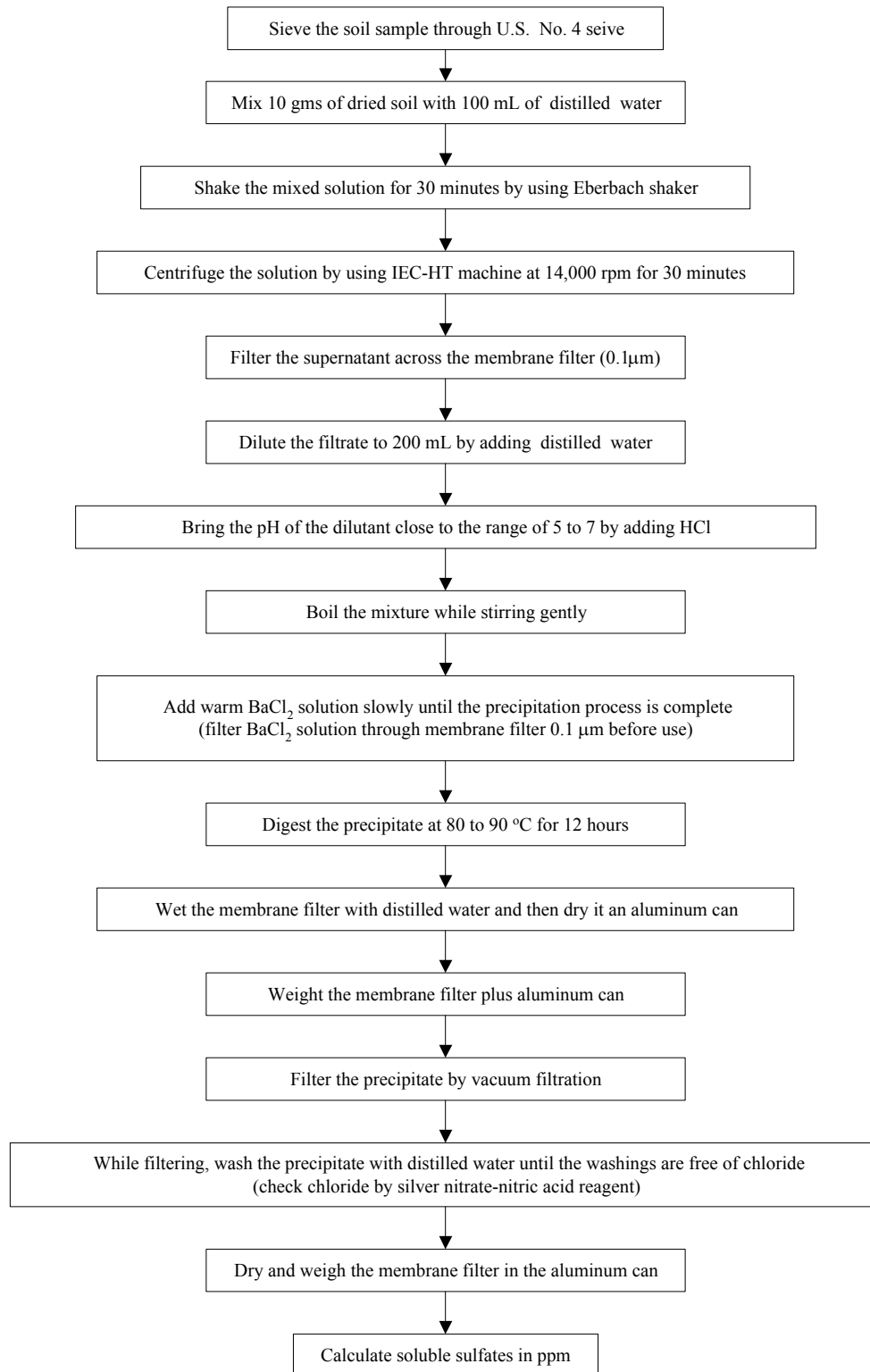
Figure 4.14 Soluble Sulfate Determination Procedures (Puppala et al., 2003)

4.6 Summary

Three distresses regions were identified based on the intensity of cracking in shotcrete lining and the limestone cores behind the tunnel lining were sampled using carbide rock core barrel and the samples were brought to UTA Geotechnical engineering laboratories. Additional care was exercised to preserve the moisture contents of the limestone core samples. Powdered sampling was done by scratching the surface of the liner material in places where white powder like substance was noticed. A series of Unconfined Compressive Strength tests (UCS), Unconsolidated Undrained Triaxial (UU) and Indirect Tensile Strength tests (IDT or ITS) were conducted using a 400 kip capacity machine. These were followed by series of X-Ray Diffraction tests (XRD), scanning Electron Microscopy Studies (SEM) and Energy Dispersive X-Ray Micro Analysis (EDAX) tests. X- Ray Diffraction Studies (XRD) were conducted in a $Cuk\alpha$ D-500 machine which uses an intense X- Ray beam. SEM studies were conducted with an accelerating voltage of 20KV and working distance less than 30. EDAX spectrums were produced using the same SEM assembly and at the same specified accelerating voltage and working distance as in the case of SEM studies. Soluble sulfate measurements were done using UTA modified approach.

CHAPTER 5

ANALYSIS OF TEST RESULTS

5.1 Introduction

The main objective of this chapter is to analyze the rock core test results obtained from engineering tests, mineralogical studies and chemical studies. The first half of the chapter is comprised of results from analyzing engineering tests namely UCS, UU, ITS and efforts were made to develop correlation between different engineering properties of limestone cores. Special emphasis was laid on point load index of limestone cores. Point load index values were back calculated from UCS point load correlations. Initial tangent modulus and secant modulus were calculated from UCS stress strain plots and correlations were developed between UCS and moduli values of limestone cores.

This chapter also presents mineralogical studies; results. Scanning electron Microscopy (SEM) images were examined to study the traces of ettringite formations in limestone cores followed by the X-ray diffraction (XRD) analyzes studies with Bragg angle concept to find the minerals including Ettringite mineral presence in the lime stone cores.

Energy Dispersive X-Ray Analysis (EDAX) studies were conducted to assess the composition of different minerals in limestone cores. Chemical studies for soluble sulfate levels were analyzed at the end to assess the amounts of soluble sulfates present in limestone cores.

5.2 Engineering Test Results and Analysis

Engineering tests namely Unconsolidated Undrained (UU), Unconfined Compressive Strength (UCS) and Indirect Tensile Strength (ITS) were conducted at UTA laboratories. The samples from the bore holes were cut and trimmed for specific aspect ratio followed in this research. For the UCS and UU tests, the specimens were cut 5.6 in. in height and 2.8 in. in diameter, and for the ITS, the length of the specimen was 2.8 in. and the diameter of the specimen was 2.8 in.

5.2.1 Unconfined Compressive Strength (UCS) Test Results

The rock cores were collected mainly from three locations namely Low Distress Region (LDR, C1 and C2), Medium Distress Region (MDR, C3 and C4) and High Distress Region (HDR, C5 and C6). Figure 5.1 presents typical UCS test results of the rock cores of each of distress region.

At each distress location two rock core samples were collected and tested for compressive strength. Figure 5.2 present average UCS test results of rock cores collected from each distress location. Table 5.1 also presents a summary of these results. The average UCS values of low, medium and high distress region rock cores are 2283, 1845 and 915 psi, respectively. These results suggest that the unconfined compression strength was low when the distress level is high and severe. This also confirms that the high distress region has low strength rock material and hence the use of UCS values for any geotechnical and structural designs should consider or account for the distress effects on the UCS strength properties.
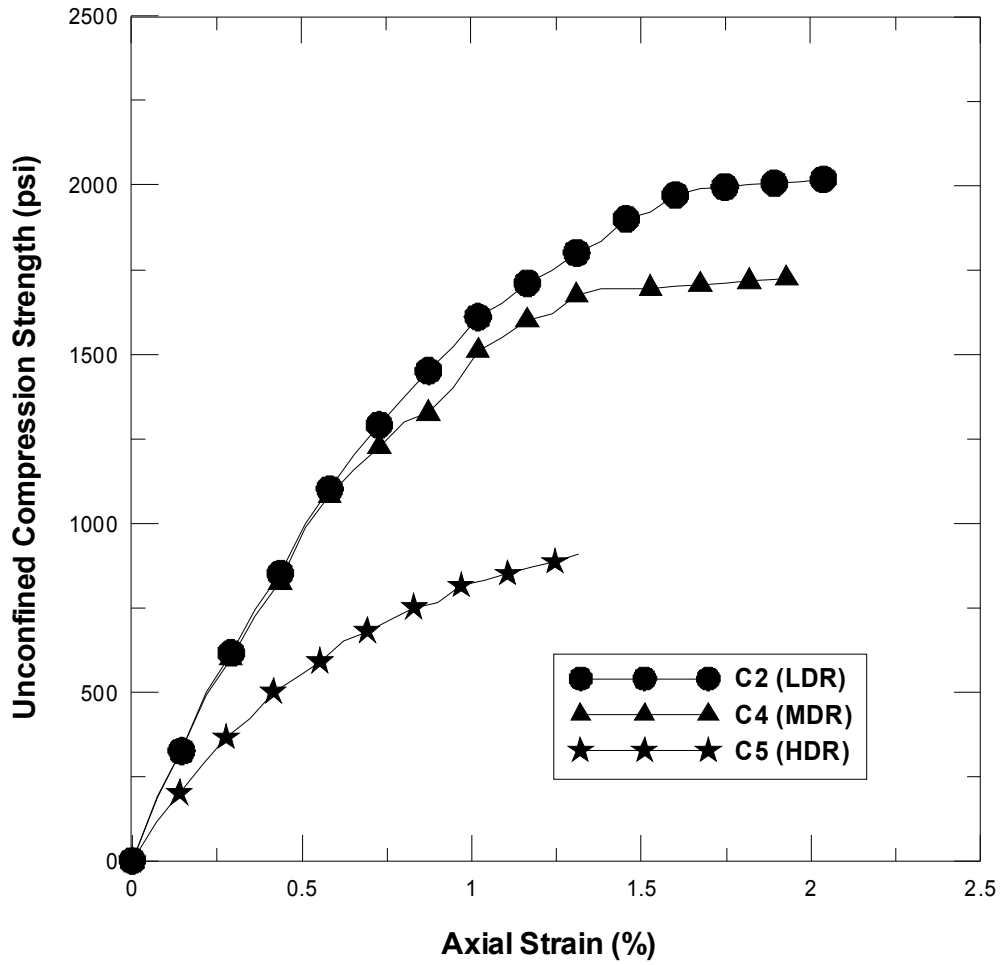
Figure 5.1 Typical UCS Test Results of Rock Core Samples from
Three Distress Regions
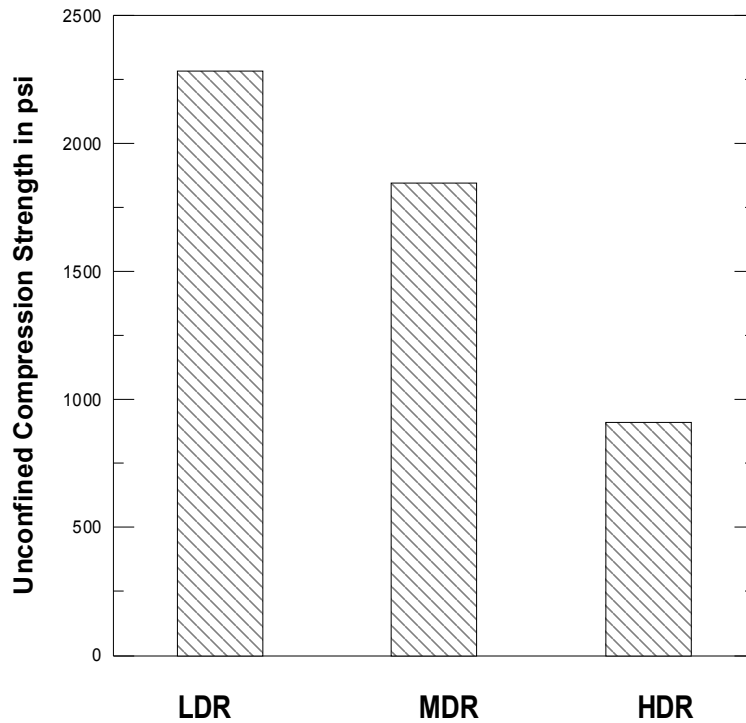
Figure 5.2 Average UCS Test Results of Limestone Core Samples

5.2.2 Unconsolidated Undrained Triaxial (UU) Test Results

All UU tests were conducted at a confining pressure of 21 psi or 150 kPa, which was to simulate a confining pressure of medium size depths of 15 ft or above. The depths at which rock cores were sampled are larger than the depths considered here. However, low confinements are still considered since the main intent of these UU test is to show whether the material exhibit any stress dependency behavior.

Figure 5.3 presents typical deviatoric stress – axial strain profiles of high to low distress rock core samples. As expected, the high distress core exhibited low deviatoric stress whereas the low distress core yielded higher deviatoric stress at failure. The secant moduli of the same material varied between 85 ksi (high distress) to 220 ksi (low

distress). Figure 5.4 shows the average UU test results for different distressed regions. All the present test results were averaged and presented in the bar chart format in Figure 5.4. Trends noted in the figure can be explained as the following:
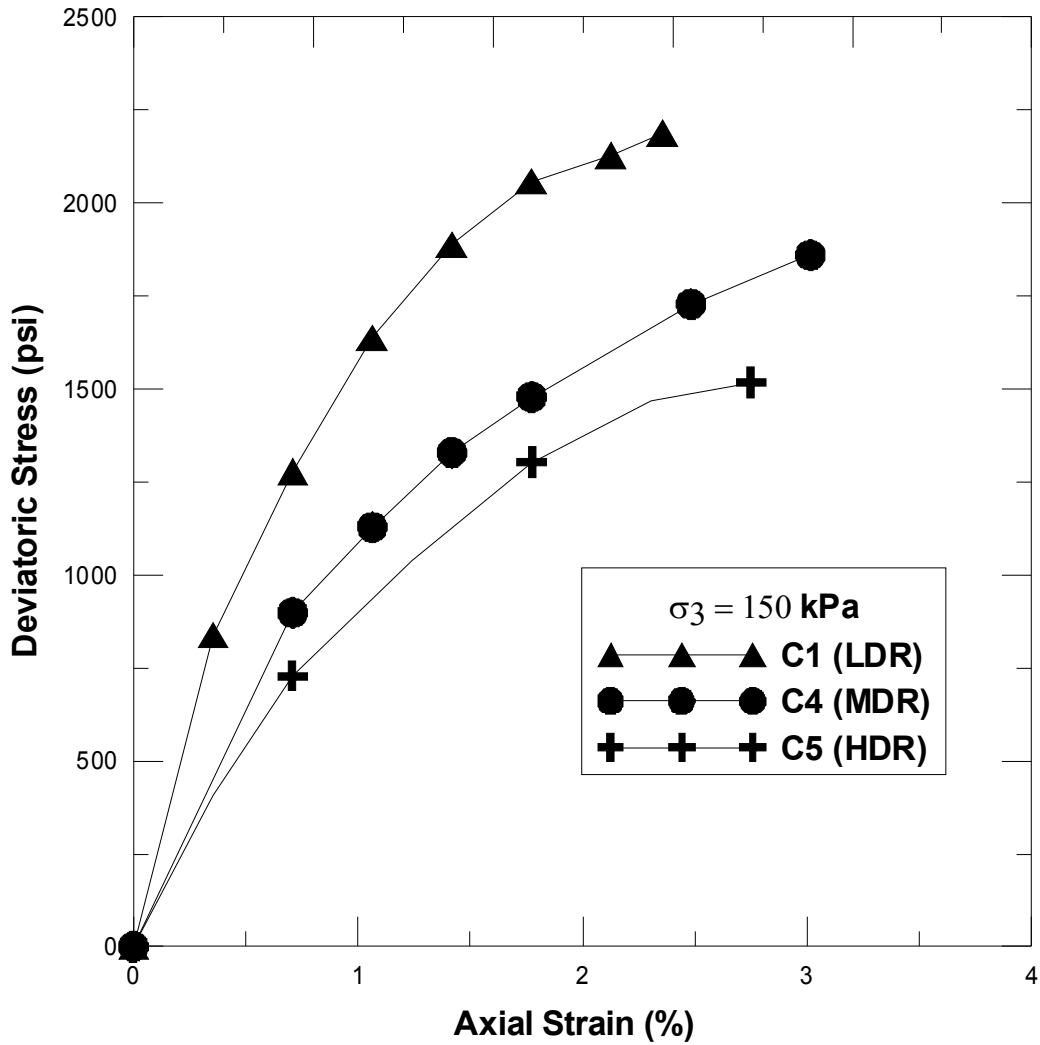
Figure 5.3 Typical UU Test Results on Limestone Core Samples

Table 5.1 UCS, UU and ITS Test Results

Core Name	UCS (psi)	Deviatoric Stress in psi (UU Test)	Load at Failure IDT (lbs)
C1 (LDR)	2551	2187	2037
C2 (LDR)	2017	1908	1901
C3 (MDR)	1966	1860	1601
C4 (MDR)	1724	1708	1563
C5 (HDR)	910	1518	900
C6 (HDR)	918	1450	880

Comparisons between UCS and UU test results as shown in Table 5.1 and Figure 5.4 indicate that medium to low distress rock cores show strength properties that are independent of applied confining pressures as these results of UU tests are in the same range as those of UCS test results. This is expected since intact rocks are not influenced by confining pressures as the bonds in the rocks are highly cemented and they tend to induce high cohesion which contributes to overall UU test related strength.

In the case of high distress cores, the UU loads appear to be influenced by the applied confining pressures as the UU strengths are much higher than the corresponding UCS values. This explains that the distressed materials due to weaker bonds can be considered as a silty sandy or granular material and hence they appear to be dependent on the confining pressures for their UU strength.
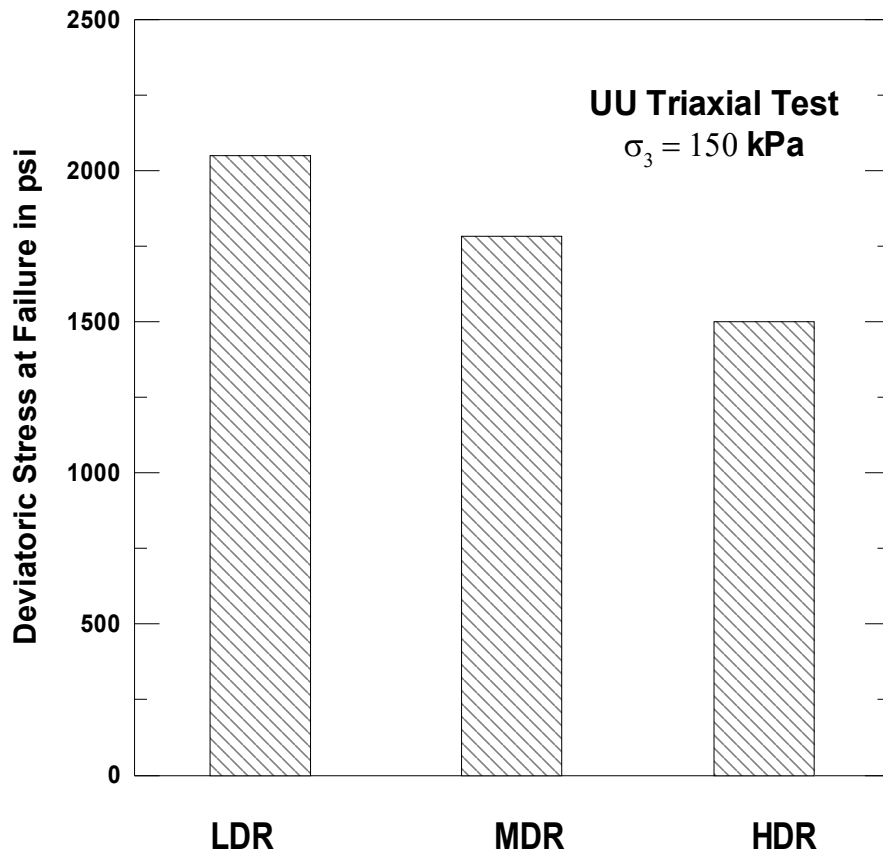
Figure 5.4 Average UU Deviatoric Load Test Results – A Comparison
(Confining Pressure of 21 psi or 150 kPa)

5.2.3 Indirect Tensile Strength Test Results (IDT)

As mentioned earlier ITS tests were conducted on specimens trimmed to an aspect ratio of 1 with a length of 2.8 in. and a diameter of 2.8 in. The peak loads at failure in IDT for specimens from various distress regions are presented in Table 5. A typical ITS value for core C1 was calculated as shown in the equation 5.1

$$ITS = \frac{2 \times P}{\pi \times L \times D} = \frac{2 \times 2037}{\pi \times 2.8 \times 2.8} = 165.5 \ psi \qquad\qquad 5.1$$

68

For the rest of the cores, the same calculations were made. Average ITS values for cores for each distress location were separately calculated and these results are presented in a bar chart format in Figure 5.5.
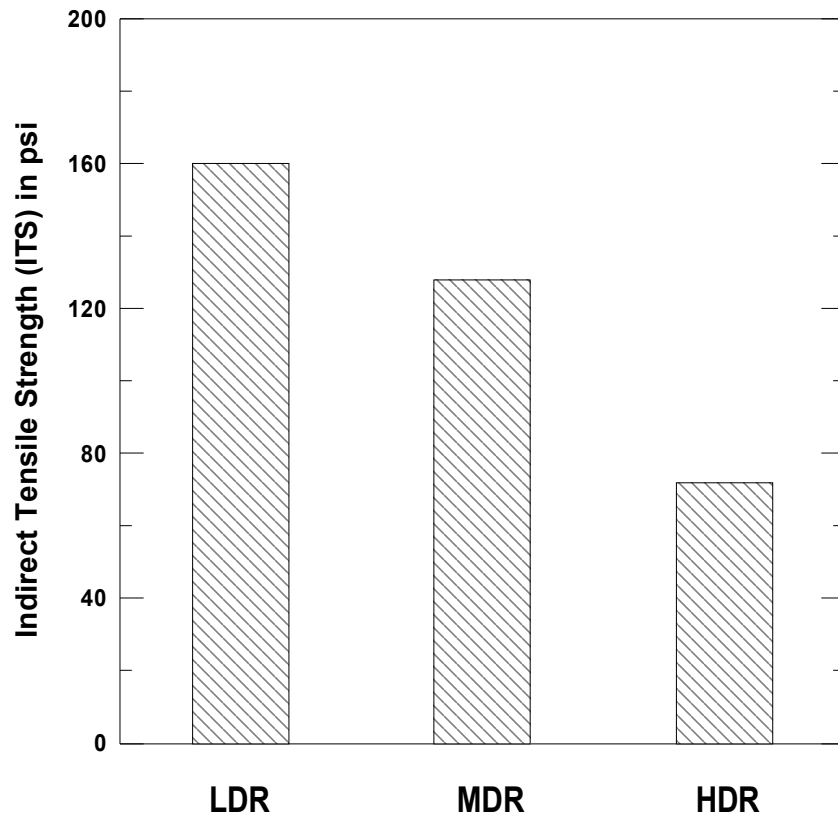
Figure 5.5 Average ITS Test Results for Different Distress Regions

The ITS values are around 160 psi for low distress rock cores to as low as 72 psi for high distress rock cores. This clearly shows that the distress location has a profound effect on the ITS values determined from the present testing. An attempt is made to correlate the tensile strength values with the average unconfined compressive strength values in the Figure 5.6. It can be seen from the figure that a good correlation exists

between UCS and ITS test results. The coefficient of determination R^2 for this correlation is around 0.99, which shows an excellent correlation is obtained between UCS and ITS. However it is important to notice that the data used for this correlation is small due to the limited number of rock specimens tested in this research, hence this correlation should be used with great care. More UCS and ITS tests on the field cores will assist in the better assessments of this correlation.
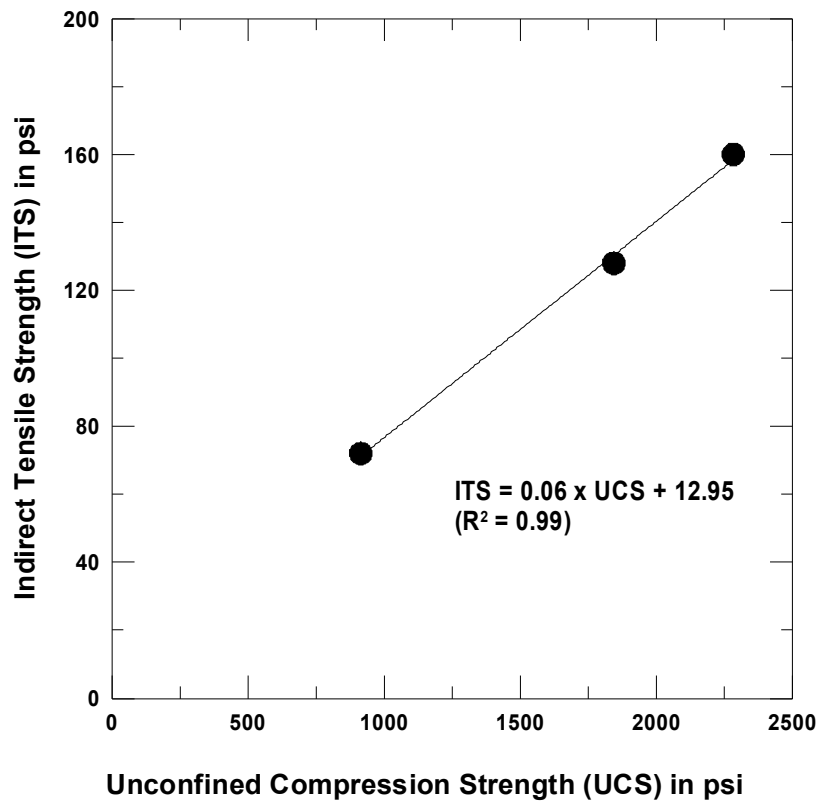
Figure 5.6 Correlation between UCS and ITS Values

5.2.4 Point Load Index from UCS Values

Point load index is an index property of rock mass and is an indirect measure of compressive strength of the rock mass. Point load strength test gives a point load index and has been found useful in rock classification and rock strength estimation. Due to its

ease of test operation, simplicity of specimen preparation and less complicated equipment, engineers often prefer this test method over uniaxial compressive strength tests. Point load index is used to estimate other index properties of rock mass including UCS, Schmidt Hammer Number, which is used to estimate the strength of the rock surface along a discontinuity (which may be weaker than body of the rock) and porosity parameter.

In the point load test, a compressive load is applied through two conical platens which cause the rock to break in tension between these two points. Figure 5.7 shows the mechanism of application of load in point load test.
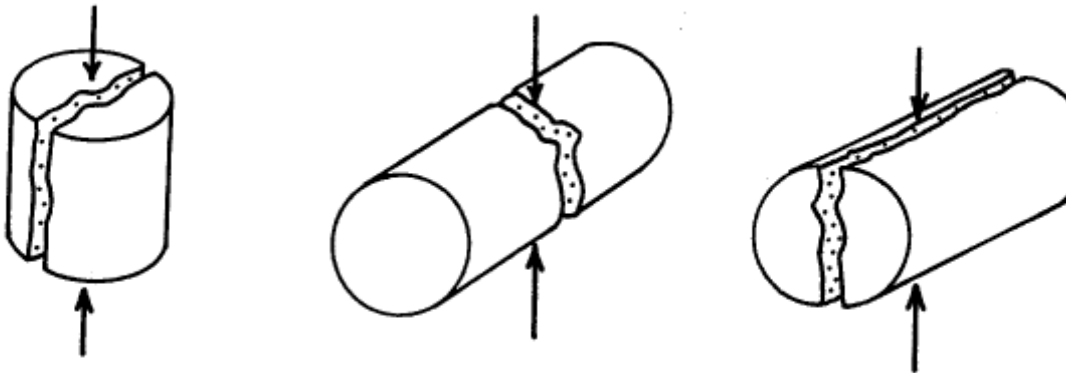
Figure 5.7 Application of Load in a Point Load Test (a) Axial Loading (b) and (c) Diametric Loading (Marinos et al., 2006)

If the breaking load is P, the point load index I$_s$ can be determined by:

$$I_s = \frac{P}{D^2}$$

5.2

Where D is the diameter of the specimen if the load is applied in the diametric direction of a core.

In other cases,
$$D = 2\sqrt{\frac{A}{\pi}}$$
5.3

Where "A" is the minimum cross-sectional area of the specimen for a plane through the platen contacts points. Values of I_s are dependent on the diameter of the sample. Value of I_s increases as diameter of specimen increases. Generally measured I_s are converted in to I_s at D = 50 mm by applying a size correction factor as presented below:

$$I_{s(50)} = I_s K_{PLT}$$
5.4

Where K_{PLT} is the size correction factor, which was determined by various researchers and has different values to it. Generally accepted equation for calculating K_{PLT} is shown below

$$K_{PIT} = \left(\frac{D}{50}\right)^{0.45}$$
5.5

In general, the point load test can be applied axially or diametrally to rock cores or to irregular lumps (Chau et al., 1996). Standard testing procedure has been suggested by American Society for Testing and Materials (ASTM) and International Society for Rock Mechanics (ISRM). Although the point load test has been studied extensively by experimental approach, there are many ambiguities about the actual stress distribution within the rock cores under applied load. However, it is usually believed that tensile failure occurs along the specimen between the opposing point loads and that the magnitude of the applied load at the instant of failure is related to both the tensile strength and the uniaxial compressive strength. The most commonly accepted formula relating the

point load strength index and the uniaxial compressive strength is that proposed by Broch and Franklin (1972).

$$q_u = 24 I_{s(50)}$$
<div align="right">5.5</div>

Where q_u is the UCS and $I_{s(50)}$ is the point load strength index corrected to a specimen diameter of 50 mm. Figure 5.8 shows typical point load test setup.

Figure 5.8 Point Load Index Test Setup (www.aimil.com)

As there were limited number of limestone samples, point load tests were not conducted. Instead point load index was calculated from UCS test results using Broch & Franklin (1972) equation. The Calculations are shown below:

For a sample diameter of 71.12 mm, size correction factor

$$K_{PLT} = (71.12/50)^{0.45} = 1.17$$

Table 5.2 Values of Point Load Index from UCS

Distress Region	Average UCS (MPa)	K_{PLT}	Average Equivalent Point Load Index (I_{50})(MPa)	Average Actual Point Load Index (I_s)(MPa)
LDR	15.74	1.17	0.66	0.56
MDR	12.72	1.17	0.53	0.45
HDR	6.30	1.17	0.26	0.22

5.2.5 Deformation Characteristics of Limestone Cores

Deformation properties of rocks or soils are important as they play a vital role in prediction of settlements and load carrying capacity of geomaterials including soils, rocks and geotextiles. In soils and rocks stress is defined simply as instantaneous force divided by the original cross-sectional area of the test specimen similarly axial strain is simply the change in test specimen length divided by the original length, usually specified as a percentage. As the test proceeds, the force required to compress the specimen increases up to some point known as the proportional limit. The slope of the curve up to this point is known variously as the elastic modulus, Young's modulus, or modulus of elasticity. If the strain is with in the elastic limit of the soil or rock, will usually return to its original, undeformed shape with some plastic deformations when the load is removed. This is referred to as elasto-plastic behavior of soils and rocks. However, if the stress is high enough, the soil or rock will permanently deform. This is referred to as plastic behavior.

The elastic-plastic limit on a stress-strain curve is the point where the behavior of the rock or soil switches from elasto-plastic to plastic.

The secant modulus on the stress-strain curve is defined as the slope of the line from the origin to specific stress state (e.g. Slope of the line drawn from origin to 50% of maximum stress). Some materials do not show linear behavior in the elastic region of the stress-strain curve, so the secant modulus must be used in calculations instead of the elastic modulus. The tangent modulus at any point on the curve is defined by ASTM as the instantaneous slope of the curve at that point.

Secant Modulus and Tangent Modulus of soils and rocks are often used to predict their stress dependent behavior. Practitioners often use these moduli in the design of structures such as embankments, shallow foundations, deep foundations, slope stability problems and pavement construction for settlement calculations. Unlike modulus of subgrade reaction and stiffness, deformation moduli are a property of material and are not dependent on the pattern of loading or the magnitude of loading.

In soils and rocks, 'Secant Modulus' and 'Tangent Modulus' values are often used in conjunction with UCS values to classify (Deere and Miller, 1966; Stagg and Zienkiewicz, 1968). As mentioned earlier secant and tangent moduli are property of material hence classification of material based on these moduli values is relatively easy and preferred by many engineers and practitioners. However a wide range of elastic moduli values can exist for a particular geologic rock type, depending upon differences in their inherent properties such as porosity, cementation, degree of weathering, formation heterogeneity, grain size angularity, and degree of interlocking of mineral grains

(Goodman, 1989). The values of secant modulus and tangent modulus also depend upon the orientation of load application with respect to microstructure (e.g., foliation in metamorphic rocks and bedding planes in sedimentary rocks.

In the present research, initial tangent modulus and secant modulus at 50% of maximum stress (E_{50}) for limestone cores from various distressed regions were calculated from the unconfined compressive strength curves. These values are reported in Table 5.3. An attempt was made to develop a correlation between compressive strength values and initial tangent (E_t) and 50% secant (E_{50}) moduli values.

Table 5.3 Comparison for Engineering Properties of Limestone of this Research

Location	Average UCS (psi)	Average Brazilian Split Tensile Strength (psi)	Average Initial Tangent Modulus, E_t (ksi)	Average (50%) Secant Modulus (E_{50}) (ksi)
LDR	2283	160	297.5	225.5
MDR	1845	123	245.8	210.5
HDR	915	72	95	85

As expected from the distress patterns lime stone cores from high distressed regions showed low initial tangent modulus values in the order of 95 ksi where as the low distress regions showed values in the order of 290 ksi. For the high distressed regions secant modulus was in the range of 85 ksi where as for the low distressed regions the values of secant modulus were in the range of 240 ksi.
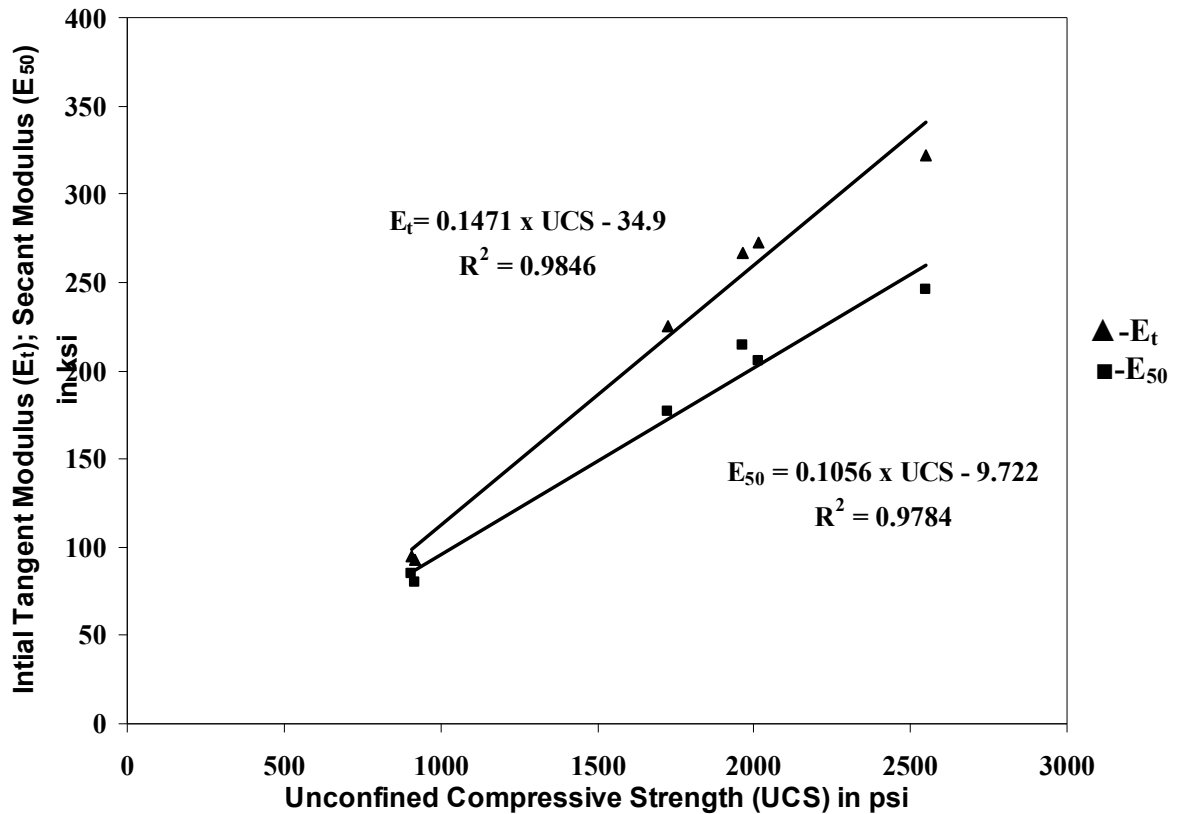
Figure 5.9 Correlations between Initial Tangent Modulus (E_t), Secant Modulus (E_{50}) and Compressive Strength of Limestone Cores

There is a strong correlation between initial tangent modulus and compressive strength of the limestone cores with a R^2 value of 0.98. Similarly there is a strong correlation between secant modulus (E_{50}) and compressive strength of lime stone cores with a R^2 value of 0.9784. However these correlations require engineering judgments as the data is limited.

Similarly there is a strong correlation between initial tangent modulus and Indirect Tensile Strength (ITD or ITS) of the limestone cores with a R^2 value of 0.97. Correlation between secant modulus (E_{50}) and Indirect Tensile Strength (ITS or ITD)

values exhibited a R^2 value of 0.9445 indicating a strong correlation between them. However these correlations require engineering judgments as the data is limited.

 str Indirect Tensile Strength (IDT or ITS) and
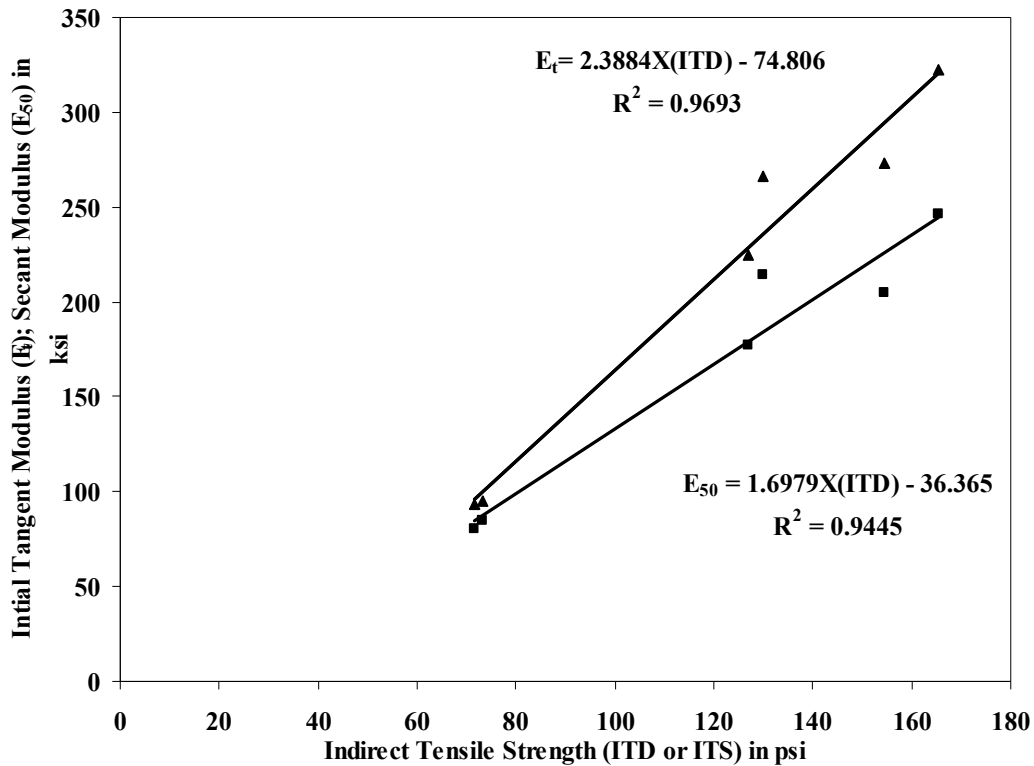
Figure 5.10 Correlations between Initial Tangent Modulus (E_t), Secant Modulus (E_{50}) and Indirect Tensile Strength (IDT) of Limestone Cores

5.2.6 Final Assessments from Engineering Test Results on Limestone Cores

Figure 5.10 shows classification of rocks based on magnitudes of compressive strength. An attempt has been made to classify the limestone cores from various distressed zones based on their compressive strengths. Table 5.4 shows the classification of lime stone core based on compressive strength values.

Table 5.4 Classification of Limestone Cores Based on UCS Values

Region	Average UCS (MPa)	Deere & Miller (1966)	Bieniawski (1973)	Broch &Franklin (1972)	ISRM (1981)	IAEG (1979)
LDR	15.7	Very Low Strength	Very Low Strength	Medium Strength	Weak	Moderately Strong
MDR	12.7	Very Low Strength	Very Low Strength	Medium Strength	Weak	Weak
HDR	6.3	Very Low Strength	Very Low Strength	Low Strength	Very Weak	Weak

From table 5.4, it is evident that limestone cores from low distressed regions are moderately strong where as the cores from medium distressed and high distress region are very weak. This phenomenon may be attributed to the distress patterns developed due to the presence swelling minerals in medium distressed regions and high distressed regions.
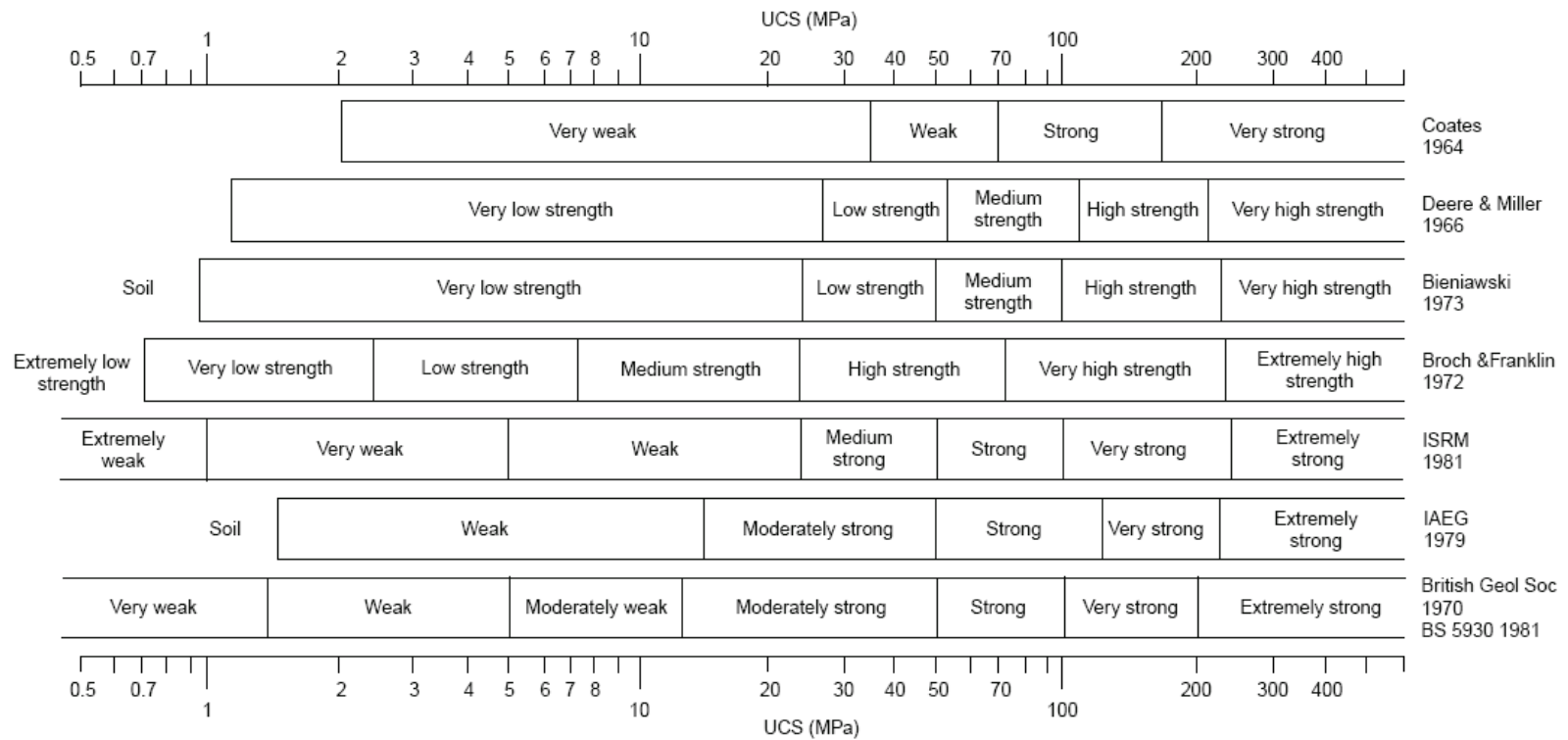
Figure 5.11 Classification of Rocks Based on Compressive Strengths by Different Authors and Organizations (Bieniawski, 1989)

It is equally important that this research examines the causes of heave related cracking in the distress zones. The DFW metroplex is known for several sulfate induced heave problems on the existing pavements. Some of these sites include State Highway 161, DFW airport taxiway, and a few other local city roads built in southern and northern regions of the metroplex. Since white powder type substance was detected in the shotcrete cracked areas (as seen in Figure 5.1b), the following systematic mineralogical and chemical studies were planned and conducted in this research. Results of these studies, which provide qualitative explanations of ettringite and thaumasite minerals, are summarized in the following sections.

5.3 Mineralogical Test Results

5.3.1 Scanning Electron Microscopic (SEM) Studies

Powder Samples prepared using carbon or copper coating as discussed earlier were samples were subjected to SEM studies and these studies did not reveal the confirmed presence of ettringite and thaumasite minerals. Figures 5.11 and 5.12 present two typical SEM pictures of low and medium distress rock core specimens. No traces of ettringite can be found in these pictures. Main reasons for the lack of detection of these minerals in these studies could be attributed to the non-existence of these minerals, or that the formed minerals could have been lost due to prolonged dry periods during which sampling was performed or due to drying of the powder specimens or due to difficulty in detecting these minerals on a tiny sample typically used for SEM studies. This SEM assessment is qualitative and hence could not be used as a sole reason for either identification or detection of Ettringite and Thaumasite minerals.
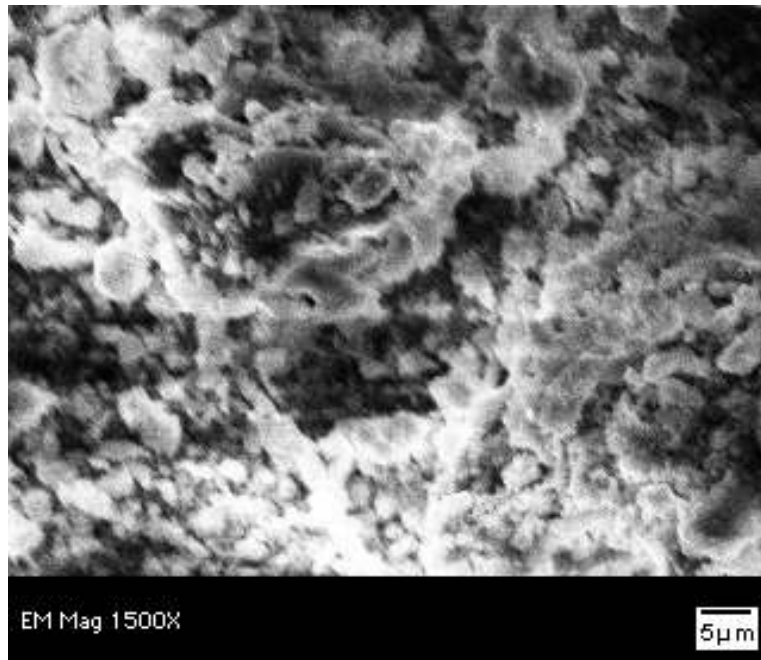
Figure 5.12 SEM Image of Powder Sample from Low Distress Area
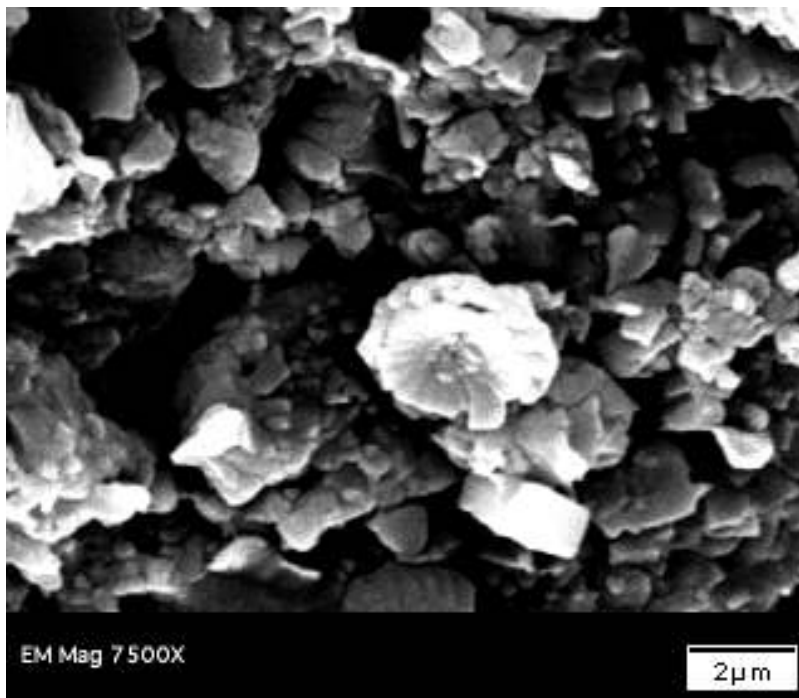
Figure 5.13 SEM Image of Powder Sample from Medium Distress Area

5.3.2 X-Ray Diffraction (XRD) Test Results

The powder samples from low, medium and high distress regions were collected and then subjected to X-Ray diffraction analysis. Figure 5.14 through Figure 5.19 presents a typical XRD data of each distress sample. Each of the basal spacing was compared with the standard basal spacings of both ettringite and thaumasite minerals and based on a reasonable match, the presence of sulfate minerals is established. This analysis results are presented in Tables 5.5 to 5.10.
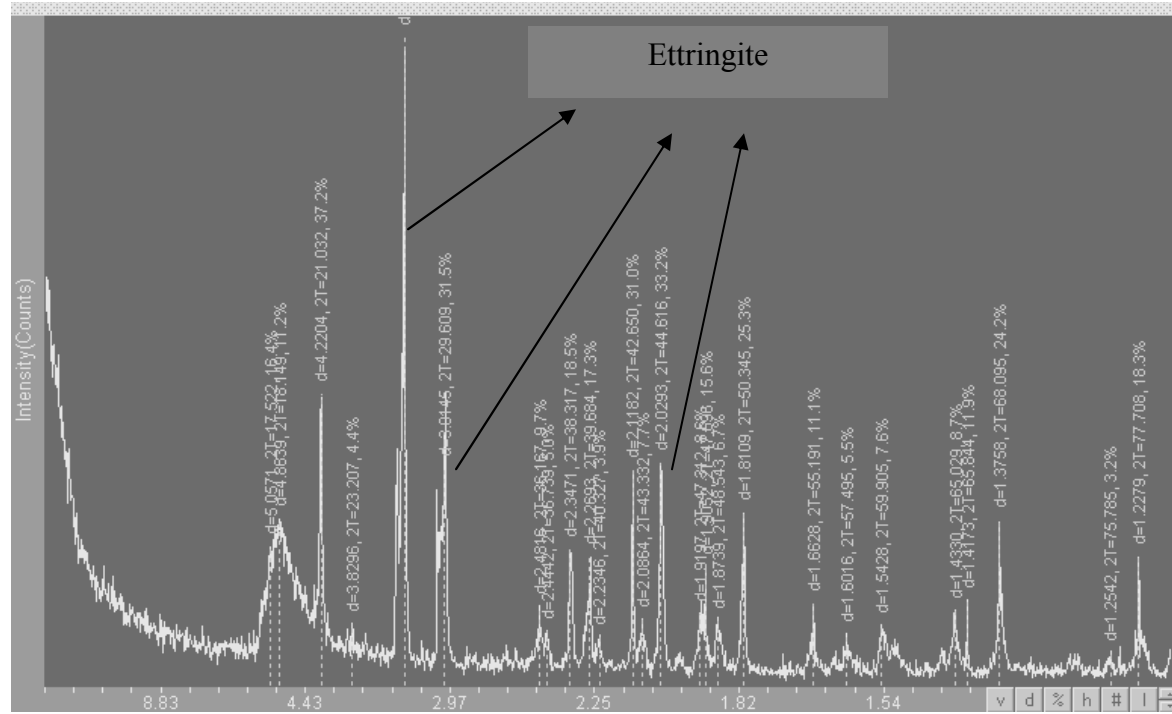
Figure 5.14 XRD Output (Basal Spacing on X axis and Intensity on Y axis)

For Low Distressed Areas
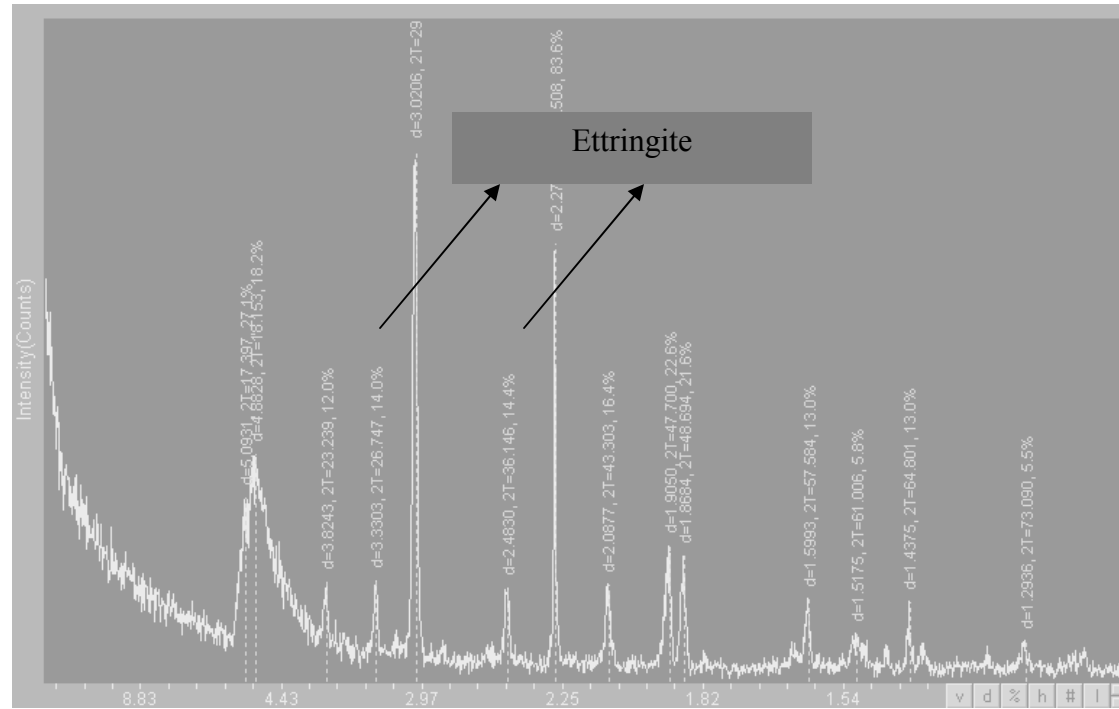
Figure 5.15 XRD Output (Basal Spacing on X axis and Intensity on Y axis)

For Low Distressed Areas
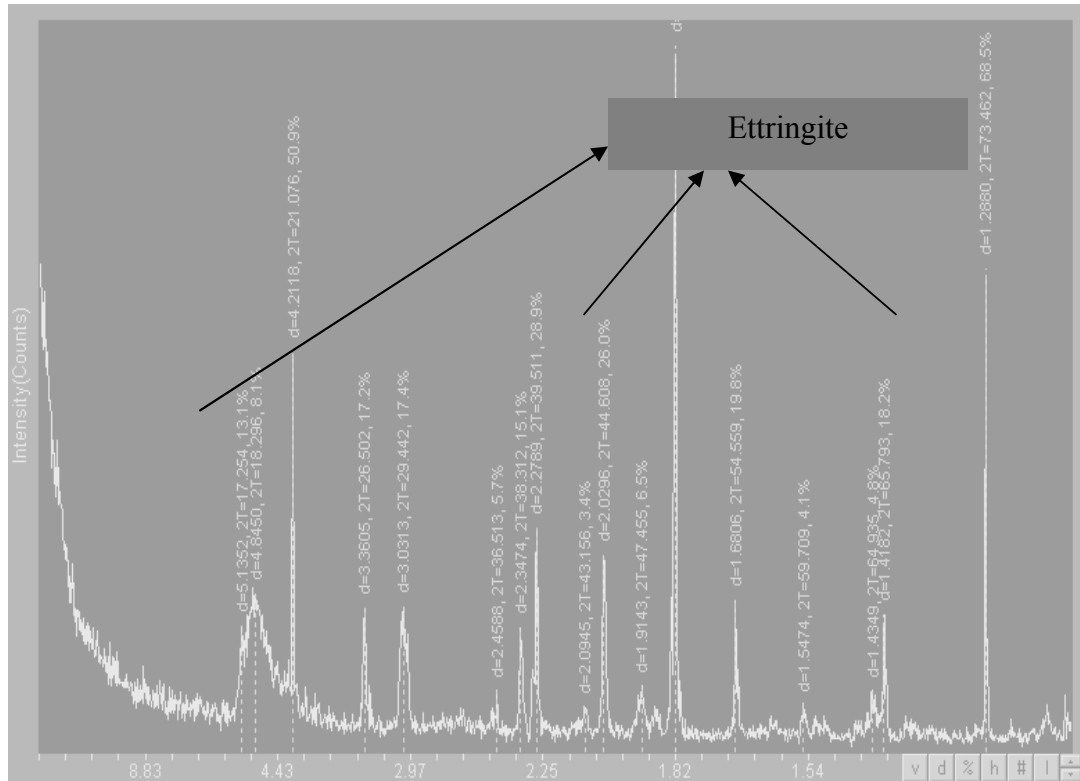
Figure 5.16 XRD Output (Basal Spacing on X axis and Intensity on Y axis)

For Medium Distressed Areas
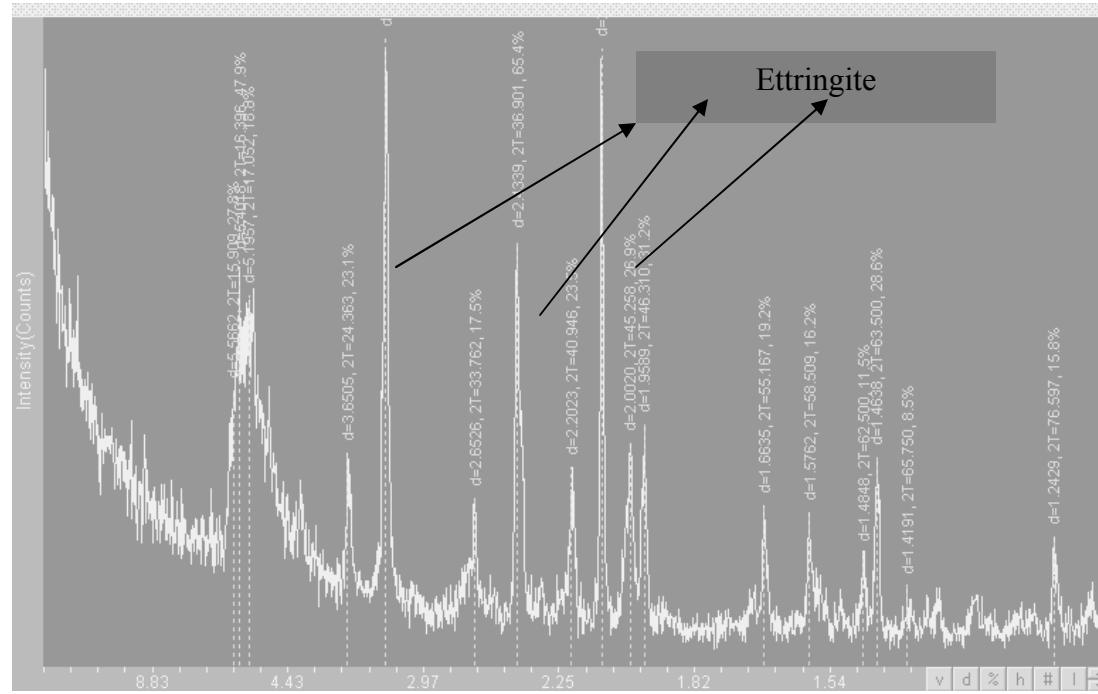
Figure 5.17 XRD Output (Basal Spacing on X axis and Intensity on Y axis)

For Medium Distressed Areas
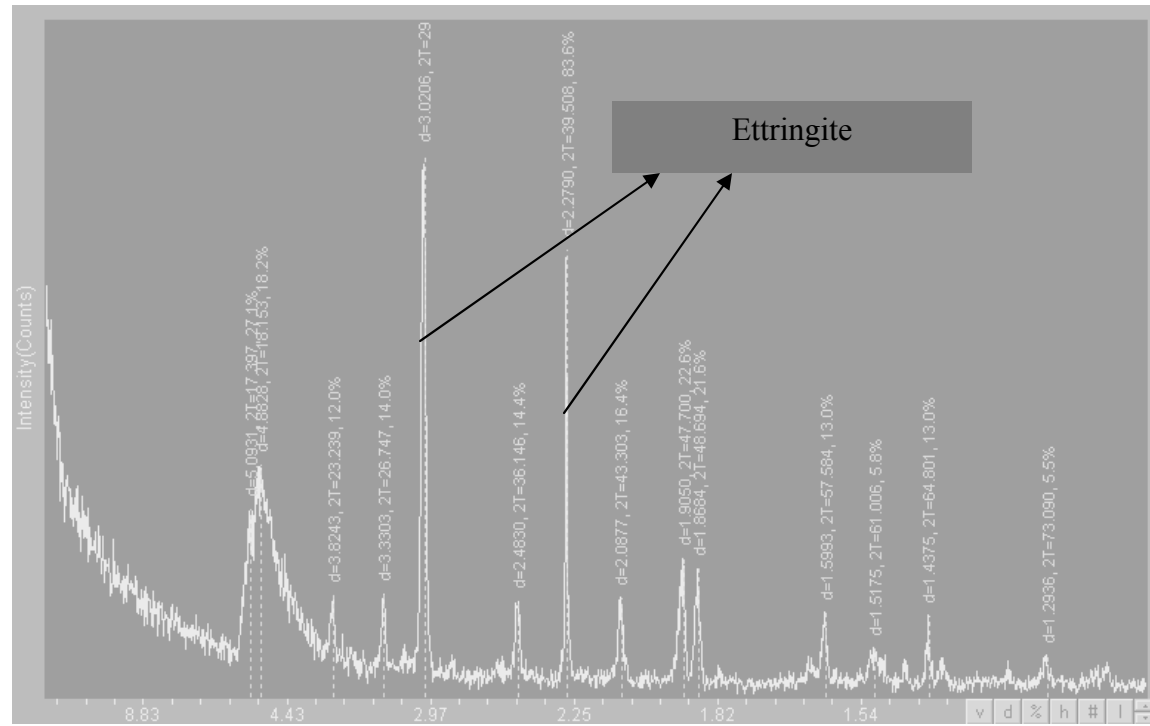
Figure 5.18 XRD Output (Basal Spacing on X axis and Intensity on Y axis)
For High Distressed Areas
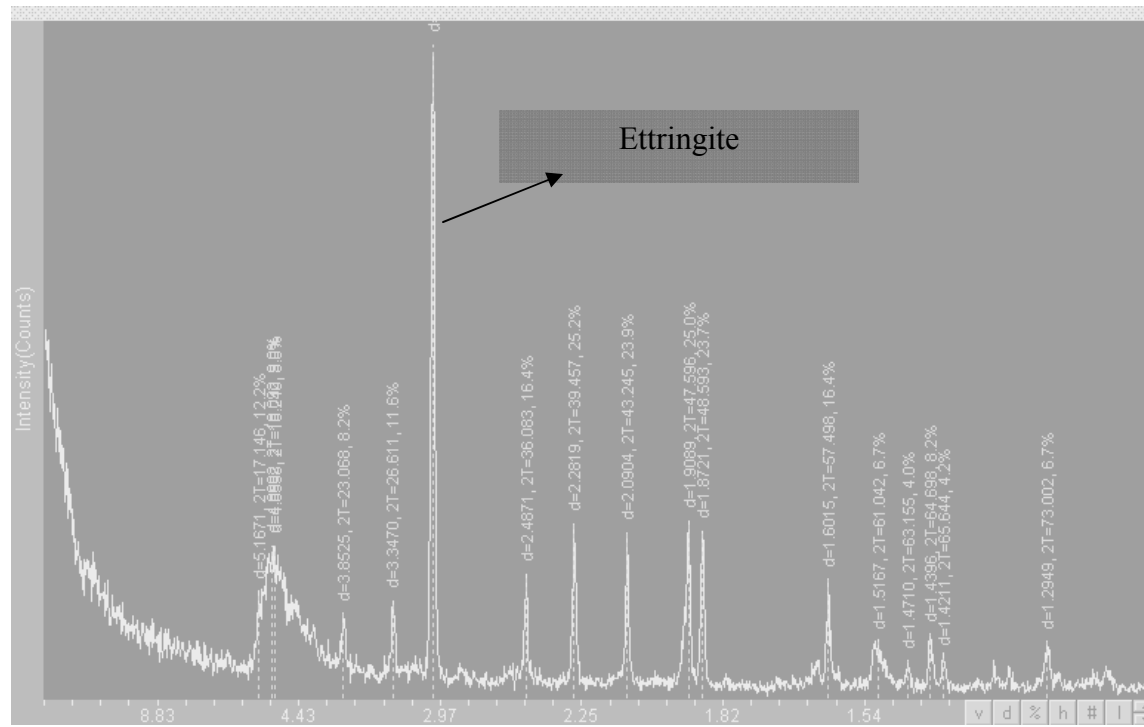
Figure 5.19 XRD Output (Basal Spacing on X axis and Intensity on Y axis)
For High Distressed Areas

Table 5.5 XRD Results from Powder Samples from Low Distress Region (Sample C1)

% Intensity	D - Spacing (A)	Kaolinite	Illite	Montmorillonite	Ettringite (1)	Ettringite (2)	Thaumasite	Prehnite
100.0	1.404	×	✓	×	×	×	×	✓
93.6	2.095	✓	✓	×	✓	✓	✓	✓
84.7	3.509	×	×	✓	×	✓	×	✓
68.5	5.258	×	×	×	×	×	×	×
66.7	3.142	✓	×	×	×	✓	×	×
61.1	2.708	×	×	×	✓	✓	✓	×
56.3	5.532	×	×	×	×	×	✓	×
42.7	3.509	×	×	✓	×	✓	×	×
38.0	1.242	×	✓	✓	×	×	×	×
34.3	1.463	✓	×	×	×	×	×	✓
29.8	1.571	✓	×	×	✓	×	×	×
27.9	1.861	✓	×	✓	✓	×	✓	✓
24.2	3.555	✓	×	×	×	×	✓	✓
21.6	1.965	✓	✓	×	✓	✓	✓	×
21.6	1.965	✓	✓	×	✓	✓	✓	×
20.2	1.955	✓	✓	×	✓	×	✓	✓
20.2	1.948	✓	✓	×	✓	×	✓	✓
17.2	1.219	×	×	×	×	×	×	✓
15.3	2.348	✓	×	×	✓	✓	✓	×
14.4	1.708	✓	✓	✓	✓	×	×	✓
9.8	1.411	×	✓	×	×	×	×	✓
9.3	1.873	✓	×	✓	×	×	✓	×
9.2	2.328	✓	✓	×	×	✓	✓	✓
6.8	2.708	×	×	×	✓	✓	✓	×
5.4	1.313	×	×	×	×	×	×	×

Table 5.6 XRD Results from Powder Samples from Low Distress Region (Sample C2)

% Intensity	D – Spacing (A)	Kaolinite	Illite	Montmorillonite	Ettringite (1)	Ettringite (2)	Thaumasite	Prehnite
100.0	3.313	×	✓	✓	×	×	×	×
59.7	2.270	✓	✓	✓	×	×	✓	×
35.7	3.015	×	×	✓	✓	✓	×	×
32.1	4.925	×	✓	×	×	×	×	×
30.2	2.029	×	✓	×	×	✓	✓	×
18.9	4.756	×	×	×	×	×	×	×
18.4	1.907	×	✓	×	✓	×	✓	×
15.3	2.345	✓	×	×	✓	✓	✓	×
12.7	1.372	×	✓	×	×	×	×	✓
12.2	1.675	✓	✓	✓	✓	×	×	✓
11.5	1.813	✓	×	×	✓	×	✓	✓
10.8	1.382	×	✓	×	×	×	×	✓
10.6	2.480	✓	✓	✓	✓	✓	✓	×
9.0	1.873	✓	×	✓	×	×	✓	×
8.7	2.450	×	✓	×	×	✓	×	×
8.5	1.435	×	✓	×	×	×	×	✓
8.1	5.173	×	×	×	×	×	×	×
7.5	4.240	×	×	×	×	×	×	×
5.5	2.088	×	✓	×	✓	✓	×	✓

Table 5.7 XRD Results from Powder Samples from Medium Distress Region (Sample C3)

% Intensity	D - Spacing (A)	Kaolinite	Illite	Montmorillonite	Ettringite (1)	Ettringite (2)	Thaumasite	Prehnite
100.0	1.822	✓	×	×	×	×	×	×
68.5	1.288	×	✓	✓	×	×	×	✓
50.9	4.212	×	×	×	×	×	×	×
28.9	2.279	×	✓	×	×	×	×	×
26.0	2.030	×	×	×	×	×	✓	×
19.8	1.681	✓	×	✓	✓	✓	✓	✓
18.2	1.418	×	✓	×	×	×	×	✓
17.4	3.031	×	×	✓	✓	×	×	×
17.2	3.361	✓	✓	×	×	×	×	×
15.1	2.347	✓	✓	×	×	✓	×	×
13.6	4.978	×	×	×	✓	✓	×	×
13.1	5.135	×	×	×	×	×	×	×
10.8	4.911	×	✓	×	×	×	×	×
6.9	4.832	×	×	×	×	×	×	×
6.5	1.913	✓	×	×	✓	×	✓	×
5.7	2.459	✓	✓	×	×	×	×	×
5.5	3.313	×	×	×	×	×	×	×
5.3	4.277	×	×	×	×	×	×	×
4.8	1.435	×	✓	×	×	×	×	✓
4.6	1.222	×	×	×	×	×	×	×
4.1	1.547	✓	×	×	×	×	×	✓
3.6	1.445	×	×	×	×	×	×	✓
3.4	2.095	✓	×	×	×	×	×	×

Table 5.8 XRD Results from Powder Samples from Medium Distress Region (Sample C4)

% Intensity	d – Spacing (A)	Kaolinite	Illite	Montmorillonite	Ettringite (1)	Ettringite (2)	Thaumasite	Prehnite
100.0	2.0943	✓	×	×	×	×	×	×
96.6	3.2748	×	×	✓	×	✓	×	✓
65.4	2.4339	×	×	×	×	✓	×	×
47.9	5.4018	×	×	×	×	×	×	×
31.2	1.9589	✓	✓	×	✓	×	✓	×
28.6	1.4638	×	×	×	×	×	×	✓
27.8	5.5662	×	×	×	×	×	×	×
26.9	2.0020	×	✓	×	×	×	✓	×
23.5	2.2023	×	×	×	✓	✓	×	×
23.1	3.6505	×	✓	×	✓	×	×	×
19.2	1.6635	✓	✓	×	✓	×	×	×
18.8	5.1957	×	×	×	×	×	×	×
17.1	5.0908	×	×	×	×	×	×	×
17.5	2.6526	×	×	×	×	×	✓	×
16.2	1.5762	×	✓	×	×	×	×	×
15.8	1.2429	×	✓	✓	×	×	×	×
11.5	1.4848	×	×	✓	×	×	×	×
8.5	1.4191	×	×	×	×	×	×	✓

Table 5.9 XRD Results from Powder Samples from High Distress Region (Sample C5)

% Intensity	D – Spacing (A)	Kaolinite	Illite	Montmorillonite	Ettringite (1)	Ettringite (2)	Thaumasite	Prehnite
100.0	3.313	×	✓	✓	×	×	×	✗
59.7	2.270	✓	✓	✓	×	×	✓	✗
35.7	3.051	×	×	×	×	×	×	✗
32.1	4.925	×	×	×	×	×	×	×
30.2	2.029	×	✓	×	×	✓	✓	×
18.9	4.756	×	×	×	×	×	×	×
18.4	1.907	✓	×	×	✓	×	✓	×
15.3.	2.345	✓	×	×	✓	✓	✓	✗
12.7	1.372	×	✓	×	×	×	×	✓
12.2	1.675	✓	✓	✓	✓	×	×	✓
11.5	1.813	✓	✓	×	✓	×	×	×
10.8	1.382	×	✓	×	×	×	×	✓
10.6	2.480	✓	✓	✓	✓	×	✓	×
9.0	1.878	✓	×	✓	×	×	✓	×
8.7	2.450	×	✓	×	×	✓	×	×
8.5	1.435	×	✓	×	×	×	×	✓
8.1	5.173	×	×	×	×	×	×	×
7.5	4.240	×	×	×	×	×	×	×
5.5	1.435	×	✓	×	×	×	×	✓

Table 5.10 XRD Results from Powder Samples from High Distress Region (Sample C6)

% Intensity	D – Spacing (A)	Kaolinite	Illite	Montmorillonite	Ettringite (1)	Ettringite (2)	Thaumasite	Prehnite
100.0	3.027	×	×	✓	✓	✓	✓	×
25.2	2.282	✓	✓	×	×	×	✓	×
25.0	1.909	✓	×	×	✓	×	✓	×
23.9	2.090	✓	×	×	×	×	×	×
23.7	1.872	✓	×	✓	×	×	×	×
16.4	1.602	✓	×	×	×	×	×	×
16.4	2.487	✓	×	✓	✓	✓	✓	×
11.6	3.347	×	✓	✓	×	×	×	×
10.1	5.191	×	×	×	×	×	×	×
10.1	4.922	×	×	×	×	×	×	×
9.0	4.899	×	✓	×	×	×	✓	×
8.7	1.295	×	✓	✓	×	×	×	✓
8.2	3.853	✓	×	×	×	×	×	×
8.2	1.440	×	✓	×	×	×	×	×
6.3	1.522	✓	✓	×	×	×	×	✓
3.8	1.508	✓	✓	✓	×	×	×	✓

As noted from the tables and figures, both ettringite and thaumasite traces are detected in all rock core powder samples. This does explain that sulfate heave could be possible at all locations. However, the distress was only severe at two locations (high distress location) and other two types (low and medium) distress did not experience any heave related problems.

5.3.3 Energy Dispersive X-Ray Microanalysis (EDAX)

EDAX or some times referred to as EDS stands for energy dispersive X-ray analysis. Basic use of EDAX is to identify minerals present in a material i.e. composition of a material. EDAX comes as an integrated feature with SEM machine and it cannot operate on its own.

The basic principle of EDAX is bombarding the material with strong source of X-ray. Bombardment of X-rays will give an EDAX spectrum which is used to identify minerals present in a material. An EDAX spectrum is a plot between energy levels and intensity counts of the peaks. Each element in the universe will have unique energy peaks; hence the elements can be easily identified. The higher the peak in a spectrum, the more concentrated the element in the specimen. In the present research, specimens were tested using EDAX technology to identify the minerals present in the various distressed locations. Figures 5.15 and Figure 5.16 present EDAX results, with various peaks showing different chemical species. From both figures, it is clearly evident that the limestone cores have all the chemical species necessary, i.e. calcium, alumina, and sulfates to produce sulfate heaving mineral, ettringite.

It is possible that the mere presence of these sulfate source minerals does not necessarily result in this type of sulfate induced heaving. Both moisture availability and sulfate source presence are still needed for enhanced crystal mineral growth formation, which could lead to heave distress and cracking in cores at the site when the sulfate minerals are subjected to moisture hydration. Because of these reasons, both soluble sulfate measurements and moisture contents of the distressed materials were measured and presented in the following section.
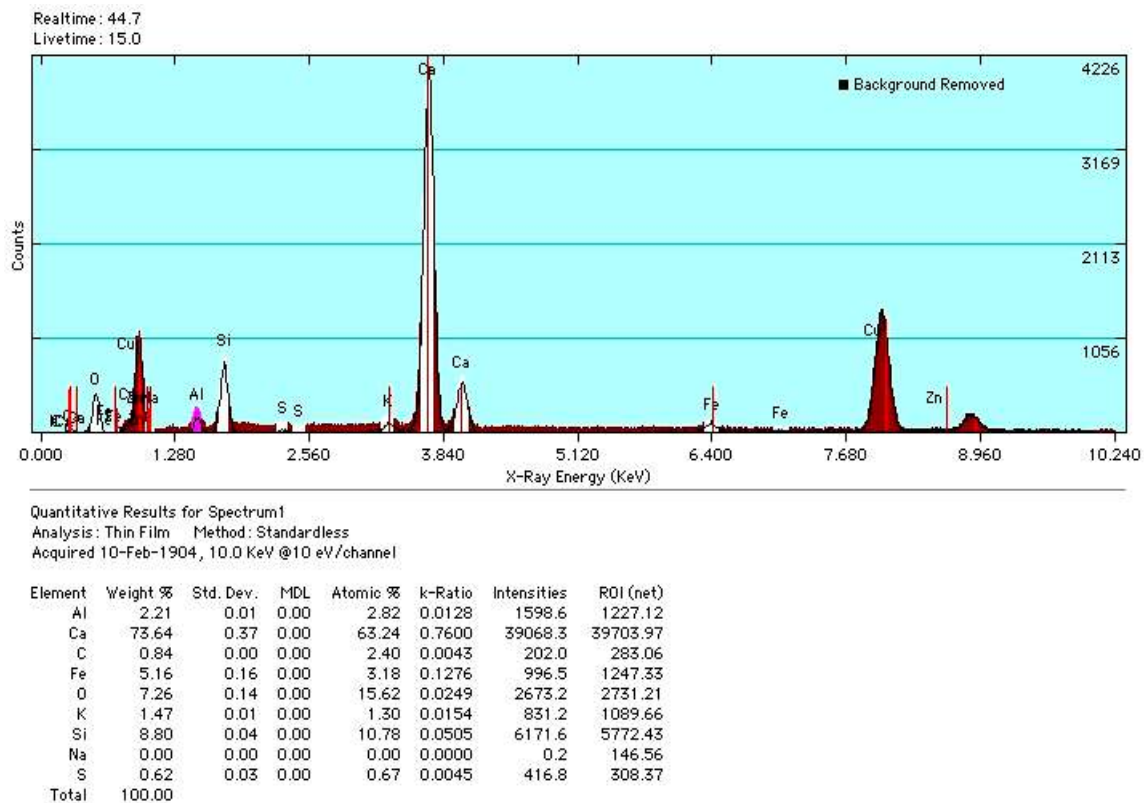

Figure 5.20 Typical EDAX Spectrums for Limestone Cores at Medium Distress Region

Realtime: 97.2
Livetime: 15.0

Quantitative Results for Spectrum1
Analysis : Thin Film   Method : Standardless
Acquired 10-Feb-1904, 10.0 KeV @10 eV/channel

Element	Weight %	Std. Dev.	MDL	Atomic %	k-Ratio	Intensities	ROI (net)
Al	1.83	0.01	0.00	2.42	0.0103	1507.3	1069.37
Ca	75.93	0.35	0.00	67.74	0.7568	45923.7	46491.21
C	0.75	0.00	0.00	2.23	0.0037	206.1	288.82
Fe	6.46	0.17	0.00	4.13	0.1499	1422.7	1798.32
O	5.15	0.11	0.00	11.52	0.0177	2164.3	2248.49
K	1.27	0.01	0.00	1.16	0.0134	816.3	1191.11
Si	7.53	0.04	0.00	9.59	0.0409	6025.8	5497.09
Na	0.00	0.00	0.00	0.00	0.0000	0.2	-7.10
S	1.08	0.04	0.00	1.21	0.0073	829.5	610.06
Total	100.00						

Figure 5.21 Typical EDAX Spectrums for Limestone Cores at High Distress Region

5.3.4 Soluble Sulfate and Moisture Content Measurements

Moisture contents of cores were measured and these values are presented in Table 5.9. High moisture contents close to 15% were measured for high distress area rock cores and low moisture contents of 4% were measured for low distress rock cores. These moisture levels are representative of the rock core conditions at the time of sampling, which was completed in the mid summer of 2006 and hence they do not address high moisture expected in spring season conditions, which typically facilitate ettringite formation.

Table 5.11 Moisture Content Details for Samples from
Various Distressed Areas

Sample Location	Average Moisture Content (%)
Low Distress	4.0
Medium Distress	13.3
High Distress	15.2

Soluble sulfate contents of powder material scratched from all rock cores were measured by using the gravimetric methodology based modified UTA method (as outlined in Figure 4.14).

Table 5.12 Soluble Sulfate Content Details for Samples from
Various Distressed Areas

Sample Location	Average Soluble Sulfate in ppm (highest sample value)
Low Distress	1,554 (1,687)
Medium Distress	2,312 (2,374)
High Distress	2,008 (2,308)

Table 5.12 presents average soluble sulfates measured along with the highest soluble sulfate value measured among each distress group cores. Sulfate levels are around

1,500 ppm at low distress location and are around 2,000 ppm at both medium and high distress locations.

It should be noted that soluble sulfates of 2,000 ppm or above are conducive enough to produce ettringite minerals in the presence of calcium compounds and high moisture conditions. As such, the present rock cores containing sulfate source minerals have formed ettringite minerals due to the presence of calcium and alumina species released from cement rich shortcrete material and rocks. Though sulfate levels and moisture contents are moderate at low distress sites, they can still induce heaving and cracking at this site, but will occur with a longer time period. This is because ettringite crystals can still form on a continuous basis and keep on accumulating (known as crystal growth) until they reach a certain threshold at which they can undergo heaving and induce cracking to rocks.

5.4 Summary

Based on the UCS, UU and ITS tests conducted on the rock cores, the following comments can be made:

All test results showed low strength values at high distress region of the tunnel. Both UCS and ITS values showed similar trends and exhibited a strong correlation between them. The UU triaxial data also showed stress independent behavior for both low and medium distress locations and a stress dependent behavior for high distress region. Values of initial tangent (E_t) and secant moduli (E_{50}) showed similar trend as the UCS values exhibiting a strong correlation. The initial tangent (E_t) and secant (E_{50}) moduli values showed considerable reduction in the case of high distress limestone core

samples. Overall, the engineering tests clearly show that the limestone cores exhibit considerable loss in strength due to distress observed at the site. As noted, the distress in the cores appeared either in the form of cracking in shotcrete material or moisture leaks

From the mineralogical studies conducted following observations can be made: Scanning Electron Microscopic studies (SEM) did not confirm the presence of ettringite crystals in the limestone core samples and powdered samples. This has been attributed to one of the following reasons

- Loss of moisture from the samples due to prolonged exposure.

- Due to pulverization techniques adopted.

- Due to absence of ettringite.

However X- Ray Diffraction (XRD) studies confirmed the presence of ettringite crystals in the limestone core samples from all the distressed regions. This was further supported by the results of energy Dispersive X- Ray Micro Analysis (EDAX) studies. Chemical studies conducted on limestone core samples also indicated soluble sulfates in the range of 2000 ppm or above for both the high distressed samples and low distressed samples. All these point to the possible presence of Ettringite mineral in the rock cores, which might have resulted in the possible cracking of material due to water adsorption. The final inference from this research investigation is that it is important to assess the sulfate levels in the sulfate rich rock cores. Otherwise, if these rocks support calcium rich shotcrete mateial, they could form ettringite, which will weaken the parent rock due to moisture hydration. As a result, liner cracking will be possible in such regions.

CHAPTER 6

SUMMARY, CONCLUSIONS AND RECOMMENDATIONS

6.1 Introduction

The main objective of the present research was to characterize the limestone cores from different distressed regions of DART NC-1B tunnel depending upon the magnitude of cracks and the water leaks. After the identification of distressed regions, affects of distress on lime stone core properties was analyzed both quantitatively and qualitatively by conducting various engineering tests and mineralogical studies. Susceptibility of limestone cores for ettringite formation was analyzed by conducting chemical tests for estimating the levels of soluble sulfates present. These tasks were successfully achieved as mentioned in the chapter 3 and 4. Some of the salient findings of this research are summarized in the following section.

6.2 Summary and Conclusions

The present research conducted on Limestone cores showed the presence of sulfates in the natural form. These sulfates formed ettringite in the presence of calcium components coming from both limestone and shotcrete material and alumina component mostly coming from cores and shotcrete material related pozzalonic compounds. Ettringite heaving caused or enhanced the cracking of the limestone behind the tunnel lining material. This heaving also resulted in cracking of shotcrete materials at locations

where ettringite formation is sufficient enough to cause this type of damage or distress. Based on the results and earlier studies reported in Chapter 2, following conclusions can be made.

1. Initial investigations of history of DART NC-1B tunnel indicated presence of several major and minor faults in limestone bedrock which is surrounded by eagle ford shale with high Pyrite and Gypsum contents. This might be the reason for the percolation of sulfate rich water through the faults encountered in the bed rock and consequent exposure of limestone cores to sulfates. In the case of shotcrete lining, sulfate rich water percolating through the bedrock might have caused the cracking in tunnel lining due the formation of ettringite and consequent high swell pressure associated with it.

2. When tested under engineering characterization methods including unconfined compression strength tests, the UCS values varied between 900 to 2000 psi for high distressed regions and low distressed regions, respectively, showing considerable reduction in the strength of limestone cores as a result of presence of sulfates. Similar trend was observed in the case of secant moduli at 50% maximum strain (E_{50}) varied from 85 to 330 ksi for high and low distressed core samples respectively. All limestone cores collected from high distress zones yielded lower strengths than those collected from low distress zones. This raises an important design concern with respect to the magnitudes of the rock properties used in the design of tunnels and tunnel liners. Typical use of factor of safety on soil properties in the geotechnical design should be able to account for the loss of

strength from the heave distress. However, this aspect still needs to be reviewed and examined.

3. It should be noted here that the present rock core sampling, which was attempted during summer months, provided cores that are representative of dry conditions in the field. Cores collected during wet or spring seasons including wet powder type materials collected during that period would have allowed additional and better screening of ettringite for more reliable evaluations of sulfate heave forming compounds. Nevertheless, the mineralogical and chemical methods used on the dry powder type of materials of the present research have provided ample proof of ettringite formation in the present core materials.

4. Two possible distress scenarios from the ettringite heaving could compromise the eventual stability of the tunnel lining material. These are: Cracking of the liner material at locations where sulfate levels are more than 2,000 ppm, and continuous moisture leaks from the cracked liner material could eventually lead to more cracking. Currently, both distresses are not considered highly problematic for the DART tunnel since the cracks are detected only at selected locations where sulfate levels are around 2000 ppm. Similar studies (as those conducted in this research) of the rock core samples collected during future spring or wet seasons will help in the better evaluation of the ettringite products formed at the site. This will also help in the better understanding of crystal growth rates of this mineral in wet season conditions, which may result in the cracking of the shotcrete liner. Wet spongy materials collected from the distress areas will

provide more insights into this heave related distress problem. Hence, researchers recommend such sampling collections in the future for the DART tunnel.

<div align="center">6.2 Remedial Measures</div>

Researchers recommend continuous monitoring of the distressed zones in other seasonal periods, which will help in performing immediate remedial works to repair the distressed zones or taking safeguard actions for preventing potential collapse of distressed zones. In the remedial works, if original shotcrete is either replaced or recoated in the distressed zones, then the researchers recommend the use of shotcrete material prepared with sulfate resistant type V cement. This is because this type of cement contains low amounts of aluminum, which will reduce the amount of ettringite formation at the project site.

APPENDIX A

SPECIMEN AND EQUIPMENT USED

Figure A.1. Preparation of Sample for Engineering Tests

Figure A.2. Shotcrete Material from Tunnel Lining

Figure A.3. D-500 Machine Operating System

Figure A.4. Representative Specimen for Austin Chalk from DART NC1 _ B Tunnel

FigureA.5 Cores of Shotcrete Material

Figure A.6 Failure of Sample in an UU Triaxial

Figure A.7 Operating System of D-500 Machine
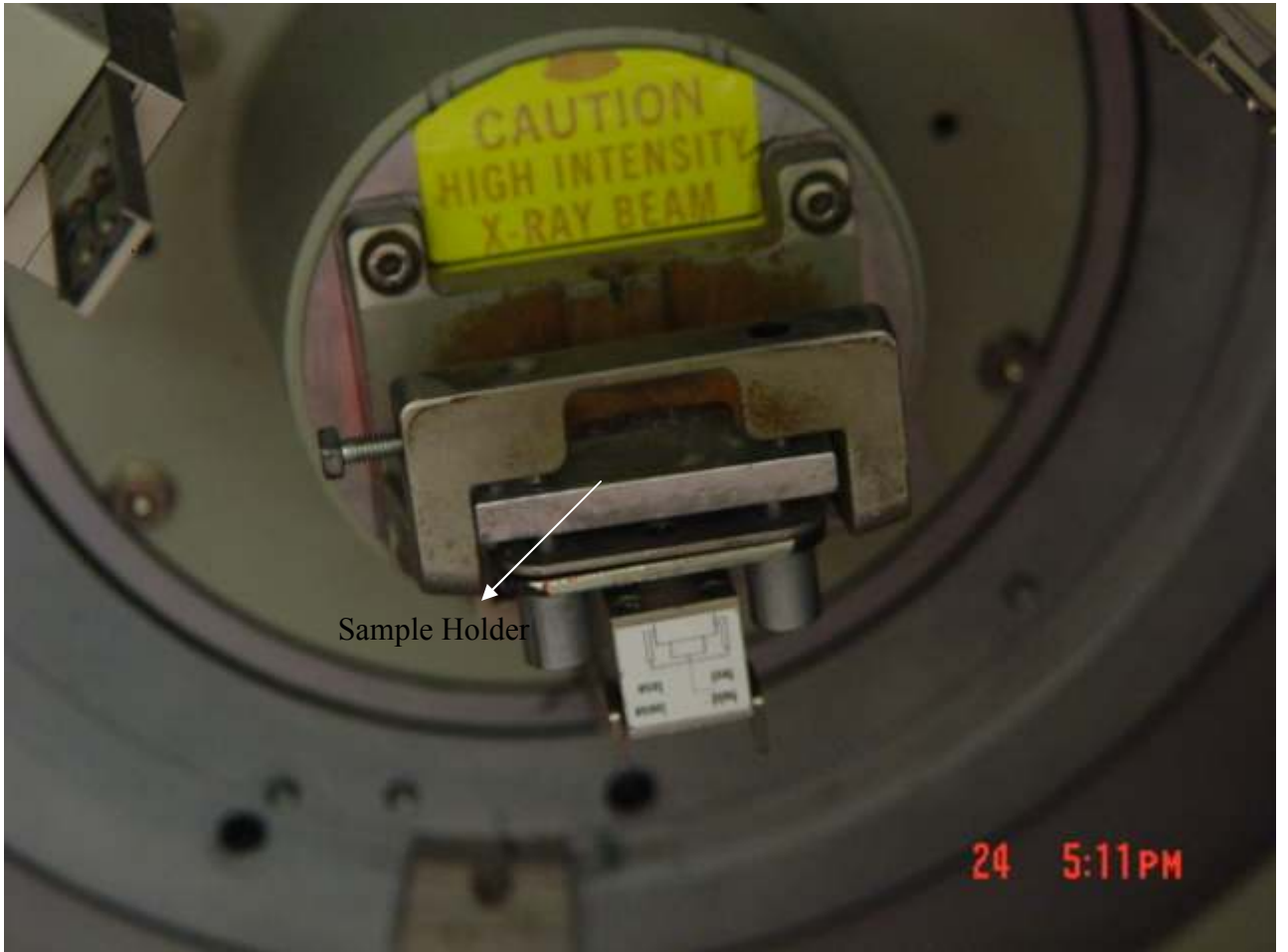
Figure A.8 Sample Ready for XRD Testing

REFERENCES

Bannerman, G.C. (2005). An Update of Sulfate Soil Management and Sulfide Issues in Road Construction. Road System & Engineering Technology Forum-August 2005, 13 p.

Basma, A.A. and Al-Sharif, M. (1994). Treatment of Expansive Soils to Control Swelling. Geothechnical Engineering, v25, 1994, pp. 3-19, ISSN: 0046-5828.

Basma, A.A., Al-Homoud, A.S., Malkawi, A.I.H. and Al-Bashabsheh ,M.A.(1996). Swelling – Shrinkage Behavior of Natural Expansive Clays. Applied Clay Science, Elsevier Science B.V, pp. 211-227.

Berdugo, I.R., Alonso. M.R. and Romero, E.E. (2006). Swelling Mechanism of Sulphate-Bearing Rocks. Presentation, EUROCK (2006), ISRM, Department of Geotechnical Engineering and Geosciences, Universitat Politecnica de Catalunya (UPC), Barcelona, Spain.

Bryant, L., Mauldon, M. and Mitchell, J.K. (2003). Impact of Pyrite and Behavior of Soil and Rock. Proceedings, 12 the Pan American Conference on Soil Mechanics and Geotechnical Engineering, Cambridge, Massachusetts, USA, v1, pp. 759-767.

Burkart, B., Goss, G., Kern, J. (1999). The Role of Gypsum in Production of Sulfate-Induced Deformation of Lime-Stabilized Soils, Environmental & Engineering Geoscience, Vol. 5, No. 2, 173 p.

Cohen, M. D., (1983). Theories of expansion in sulfoaluminate–type expansive cements: schools of thought. Cement and Concrete Research, Vol. 13, pp. 809-818.

DePuyG. W. (1994). Chemical resistance of concrete. Significance of tests and properties of concrete and concrete-making materials, ASTM 169C, P. Klieger and J. Lamond, eds., ASTM, West Conshohocken, PA, pp. 263-281.

Dermatas, D. (1992). "An Experimental Study to Elucidate and Eliminate Ettringite-Induced Swelling in Lime-Stabilized Sulfate-Bearing Clayey Soils," Ph.D. Thesis, The University of California at Berkeley, Berkeley, California, USA.

Dermatas, D. (1995). "Ettrigite-induced Swelling in Soils: State-of-the-art," Applied Mechanics Rev, Vol. 48, No. 10, pp. 659-673.

Freeman, E.T. (2003). Forensic Investigation of Pavement Distress: Old Airport Road in Bristol, Virginia. Research Report, Sponsored by VDOT and University of Virginia, 15 p.

Harris, P. (2004). Hydrated Lime Stabilization of Sulfate-Bearing Soils in Texas. Research Report, 0-4240-2, Sponsored by TXDOT and FHA 46 p.

Hunter, D. (1988). Lime-induced heave in sulfate-bearing clay soils. Journal of Geotechnical Engineering, Vol. 114, No. 2, pp. 150-167.

Hunter, D. (1989). Geochemistry of Lime Induced Heave in Sulfate Bearing Clay Soils. Ph.D. Dissertation, University of Reno, NV.

Jethwa, J.L., Singh. B., Singh, B. and Mithal, R.S. (1977) Rock Pressure on Tunnel Lining in Swelling and Viscous Rocks. Proceedings – Annual Aleerton Conference on Circuit and System Theory, 1977, pp. 45-50.

Little, D. N., and Deuel L., (1989). Evaluation of sulfate-induced heave at Joe Pool Lake. Chemical Lime Company, June

Madsen, F.T. and Nuesch, R. (1991). The Swelling Behavior of Clay-Sulfate Rocks. Proceedings – Congress of the International Society for Rock Mechanics, 1991, pp. 285-288.

Mehta, P. K., and Klein, A. (1966). Investigation on the hydration products in the system4CaO·3Al2O3·SO3 – CaSO4 – CaO –H2O", Hwy. Res. Board Spec. Rep. No. 90, NationalResearch Council, Washington, D.C. pp.328-352.

Mehta, P. K., and Hu, F. J. (1978). Expansion of ettringite by water absorption. Journal of American Ceramic Society, March/April, pp. 179-181.

Mitchell, J. K. (1986). Practical problems from surprising soil behavior. Journal of Geotechnical Engineering, Vol. 112, No. 3, pp. 259-289.

Moore, A. E., (1970). Crystal structure of ettringite. Acta Crystallographica, Vol. B26, pp. 386-393.

Moore, D. M., and Reynolds, R. C., (1989). X-ray diffraction and the identification and analysis of clay minerals, Oxford University Press, NY.

Natarajan, S.K. (2004). An Integrated Approach To Predict Ettringite Formations I Sulfate Soils and Identifying Sulfate Damage Along SH 130. A Thesis, Submitted to Texas A&M University, 2004, 156 p.

Nettleton, W. D. (1982). Gypsiferous soils in the Western United States. SSSA Special Publication No. 10. Soil Science Society of America, Madison, Wis.

Perrin, L. (1992). Expansion of lime-treated clays containing sulfates. Proc., 7th Int. Conf. On Expansive Soils, Vol.1, ASCE Expansive Soils Research Council, New York, pp. 409-414.

Prommersberger, G. and Kuhnhenn, K. (1989). The Fredenstein Tunnel: Tunnel Construction in Swelling Rocks, Proceedings-Rapid Excavation and Tunneling Conference, 1989, pp. 678-700.

Richters, G., Hood, C. and Lundin, T.K. (1999). Design and Construction of the DART Starter Line Tunnel Contract NC-1B, Dallas, Texas. Proceedings, Third National Conference, Geo - Engineering for Underground Facilities, Geotechnical Special Publication No. 90, pp. 582-594.

Rollings, R.S., Burkes, J.P. and Rollings, M.P. (1999). Sulfate Attack on Cement-Stabilized Sand, Journal of Geotechnical and Geoenvironmental Engineering, v125, No. 5, pp. 364-372, Paper No.15979.

Romer, M., Holzer, L. and Pfinner, M. (2001). Interaction of water with concrete: Deterioration Mechanism, CONSEC'01: Concrete under Severe Conditions (eds. Banthia, N. et al.) pp. 1075-1082 (Vancouver, BC. Canada, 2001).

Sherwood, P. T., (1958). Effect of sulfates on cement-stabilized clay. Highway Research Board Bulletin. 193, National Research Council, Washington, D.C. pp.45-54

Sherwood, P. T., (1962). Effect of sulfates on cement and lime-stabilized soils. Highway Research Board Bulletin, 353, National Research Council, Washington, D.C. pp. 98-107.

Taylor, H. F. W. (1974). Crystal chemistry of Portland cement hydration products. Proceedings, The Sixth International Congress on the Chemistry of Cement, Vol. II –Book 2, Moscow, 46 p.

Wang, L. (2003). Cmentitious Sabilization of Soils in The Presence of Sulfates. A Dissertation Submitted to Graduate Faculty of the Louisiana State University and Agricultural and Mechanical College, 2003, 117 p.

Wild, S., Kinuthia, J.M., Jones, G.J. and Higgins, D.D. (1998). Suppression of Swelling Associated with Ettringite Formation in Lime Stabilized Sulphate Bearing Clay Soils by Partial Substitution of Lime with Ground Granualated Blastfurnace Slag. Engineering Geology, Elsevier Science B.V. pp. 257-277.

Zanbak, C., and Arthur, C. R., (1986). Geochemical and Engineering Aspects of Anhydrite/Gypsum Phase Transitions: Bulletin of the Association of Engineering Geologists, No. 4, pp. 419-433.

BIOGRAPHICAL INFORMATION

Vivekananda Chikyala was born in Rayadari, Andhra Pradesh, India on the 20th of July, 1982. He received his B. Tech Degree from the Jawaharlal Nehru Technological University College of Engineering, Hyderabad, India in June, 2004. The author joined the University of Texas at Arlington in August, 2005 as a MS candidate in Geotechnical Engineering. During the course of his study the author worked as a graduate research assistant and teaching assistant under Dr. Anand J. Puppala and had a chance to work in various research projects involving pavement stabilization, monitoring and Sulfate induced heave in Tunnels. The author's research interests include Stabilization of expansive soils and rocks, Design of Pavements and Geotechnical Engineering Related Ground Improvement Methods.